Experimental geoecology

Fiaizullina R.V., Kuznetsov E.V., Salavatova D.S. Sorption properties of synthetic silicon organic sorbent PSTU-3F on mercury

M.V. Lomonosov Moscow State University, Department of Geology, Moscow fiaizullina@geol.msu.ru

Abstract. The possibility of using synthetic silicone sorbent PSTU-3F for the adsorption removal of mercury from an aqueous solution has been studied. The dependence of mercury adsorption on the pH of the solution, the amount of the adsorbent and the duration of the contact of the solution with the adsorbent was investigated. It was shown that the amount of adsorption is the higher, the higher the acidity of the solution. This is due to the absolute dominance of the cationic form of the bivalent mercury Hg^{2+} and the negative charge of the surface of the sorbent. It has been established that an increase in the mass of the sorbent has a significant effect on the shift of the pH of the solutions to a more alkaline region. Therefore, the optimal ratio of the sorbent - solution should be considered the ratio of 1:1000. To interpret the equilibrium mercury adsorption data, an experimental adsorption isotherm was constructed, which was analyzed using the Langmuir and Freundlich equations. As a result, it was shown that the Freundlich equation describes the adsorption process significantly better than the Langmuir equation.

Keywords: *mercury adsorption, synthetic silicon organic sorbent, adsorption isotherms, Langmuir equation, Freundlich equation.*

Mercury and its compounds are an integral part of the environment, where they are usually found in extremely low concentrations. Analytical chemistry of mercury has visibly made a step forward over the last fifty years. However, there still exist natural reservoirs in which concentrations cannot be directly determined. In such cases, one solution is to use various kinds of synthetic sorbents that significantly lower the detection limit for mercury. An additional advantage of their use is the possibility of transporting accumulated mercury on the sorbent from the sampling site directly to the measurement site, i.e. in an equipped analytical laboratory. In areas with increased anthropogenic load, another problem is particularly acute, associated with elevated concentrations of this element. A large amount of data on the negative effects of mercury on the environment, including ours (Fiaizullina et al., 2017), indicates the need for industrial and wastewater treatment. In the absence of control and reliable protective devices, it enters the soil, surface and groundwater, and bottom sediments, having an extremely negative impact on the environment. In particular, entering the aquatic ecosystem, mercury accumulates and transforms in each subsequent link in the food chain, reaching the maximum content at its top. Analysis of currently existing methods of purification of natural and waste water from heavy metals showed that one of the most promising is the sorption method. The synthetic sorbent PSTU-3F, synthesized by a group of scientists from the A.E. Favorsky Irkutsk Institute of Chemistry SB RAS under the leadership of academician M.G. Voronkov, fits the role of a sorbent capable of providing a solution to these two diametrically opposite problems. The sorbent is a spatially cross-linked organosilicon polymer with thiocarbamide groups - poly [N, N '- bis (3-silesquioxanylpropyl) thiocarbamide] (PSTU-3), which is obtained by hydrolytic polycondensation in an aqueous medium at 90-100 °C N, N'-bis- (3-Triethoxysilylpropyl) thiocarbamide (Voronkov et al., 1991):

$$n\,[(C_2H_5O)_3SiCH_2CH_2CH_2NH]_2C{=}S + 6n\,H_2O \xrightarrow[-6n\,C_2H_5OH]{} \rightarrow (O_{1,5}SiCH_2CH_2CH_2NHC(S)NHCH_2CH_2CH_2SiO_{1,5})\,n$$

Its distinctive feature is increased thermal and chemical stability, which allows operation in aggressive environments. High chemical stability allows this sorbent to function in a wide range of acidity of the medium: from pH 12 to strong concentrated acids (Vasilyeva et al., 2010). Thus, the purpose of our work was to study the sorption properties of the PSTU-3F silicone sorbent on mercury. A number of factors can influence the course of adsorption: the amount of the adsorbent, the time of its contact with the solution, the temperature and the pH value. The laboratory air temperature throughout all experiments was 24.0±1.5 °C. To measure the equilibrium concentration of mercury, the “cold vapor” method was used with an atomic absorption spectrometry using Portable Mercury Analizer PMA-1 (EcON, Moscow) with a PAR-3m attachment. The reducing agent was a 1% solution of sodium borohydride in a 1% solution of sodium alkali. To control the acidity of the solutions, the pH meter Expert-001 (Econix-Expert, Moscow) was used. A combined glass electrode “EGC-10601” (Measuring equipment, Moscow) was used as a pH electrode. The concentration of adsorbed mercury was determined by the difference of concentrations in solutions by the equation:

$$q_e = \frac{(C - C_e)\cdot m_{sol}}{m_{sorb}},$$

where q_e is the amount of Hg(II) adsorbed at equilibrium is (mcg/g); C and C_e are the initial and equilibrium concentrations of metal ions in the solution respectively (ppm); m_{sol} is the mass of the solution (g); m_{sorb} is the mass of adsorbent (g).

Effect of pH. The acidity of the solution is one of the most important parameters controlling the absorption of heavy metals. In the case of PSTU-3F, we have shown that the process of mercury adsorption is most significant in the region of more acidic pH values (Fig. 1).

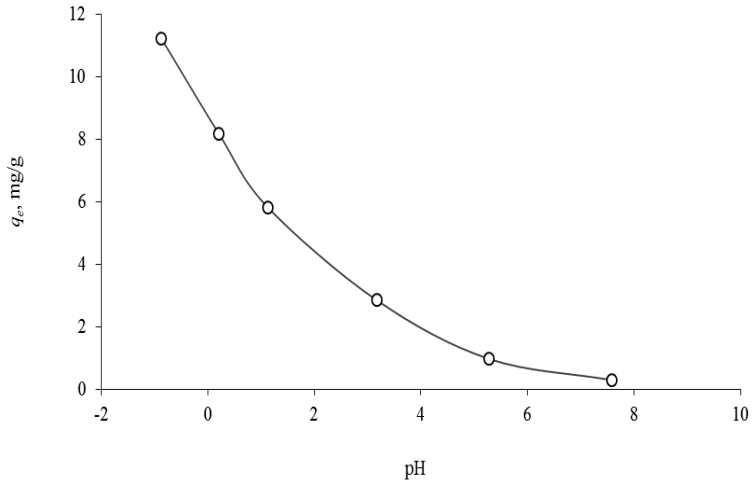

Fig. 1. Effect of pH on mercury (II) adsorption

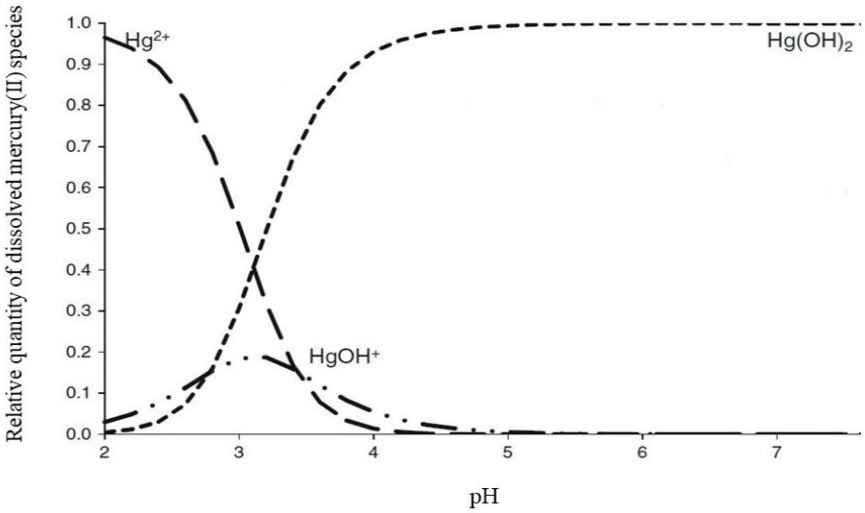

Fig. 2. The relative quantity of mercury (II) species (Nazarenko et al., 1979)

This is due to the dominance of the cationic form of mercury-divalent mercury Hg^{2+} in the area of strongly acidic solutions. This fact can be judged from the book (Nazarenko et al., 1979) on the hydrolysis of metal ions in highly diluted solutions (Fig. 2). It should also be noted that pH_{PZC} (points of zero charge) is probably in the near neutral medium, and the PSTU-3F sorbent, in the area under study, is a cation exchanger, i.e. negatively charged (Fig. 3).

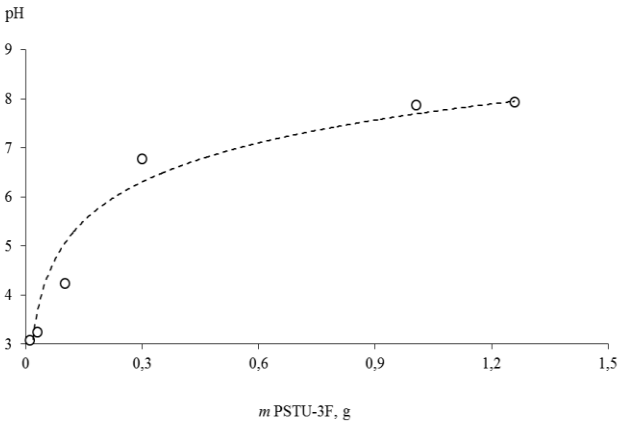

Fig. 3. The effect of the amount of sorbent on the pH of the solution

Therefore, Hg^{2+} cations are involved in the formation of the electric double layer, occupying the absolute majority of adsorption centers as a result of competing adsorption. The decrease in the amount of adsorbed substance, when shifted to the near-neutral and weakly alkaline zones, is associated with a decrease in the concentration of the Hg^{2+} particle, and in the region around the pH value equal to 3, the isoelectric point is located, in which the dominant form changes: the concentration of mercury (II) $Hg(OH)_2^0$ increases, having no charge, and, therefore, not able to be sorbed on the negatively charged surface of the sorbent. From Figure 3 the following fact also becomes obvious: with an increase in the amount of sorbent in solution, the acidity of the latter shifts to a more alkaline region. This can be explained by the formation of a double electric layer from the negatively charged surface of the sorbent, and positively charged protons attracted to it. It is obvious that with an increase in the amount of sorbent in the solution, the adsorption also increases, due to an increase in the sorbing surface. Consequently, due to the increase in the content of OH^- groups in the solution, the pH shifts to the alkaline region.

Adsorption kinetics. It should be noted that all the adsorption experiments described in this work were

carried out under static conditions (without using shakers, i.e. without active mixing). Samples were mixed by hand for 2 minutes once a day. Under such conditions, equilibrium was achieved in less than a day, and the degree of mercury recovery from solutions in this case was more than 95%.

Adsorption isotherms. Analysis of adsorption isotherms allows you to set the features of the process, to assess the feasibility of the practical use of the sorbent to absorb any substances. In this work, isotherm analysis was performed using well-known equations: Langmuir and Freundlich. As a result, an experimental adsorption isotherm was constructed, as well as isotherms recalculated using the above equations (Fig. 4). The parameters of adsorption isotherms calculated by the Langmuir and Freundlich models are listed in Table 1.

Table 1. The parameters of adsorption isotherms calculated by two different models

Isotherm	Constants	Values	R^2
Langmuir	q_m, mg/g	5.57	0.9817
	K_L	0.0082	
Freundlich	n	1.508	0.9932
	K_F	0.1025	

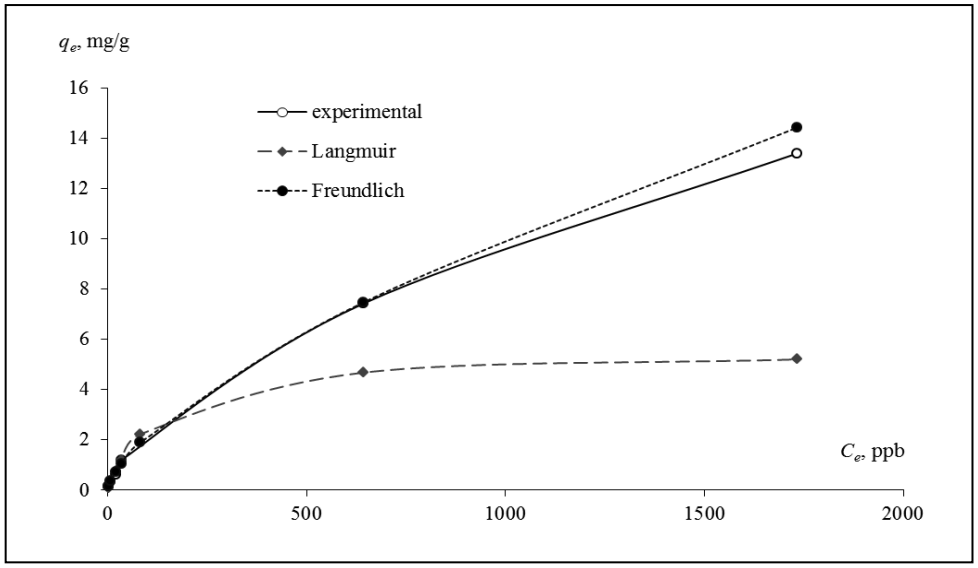

Fig. 4. Isotherms of mercury adsorption on PSTU-3F sorbent

From the data obtained, it becomes obvious that the most accurately studied adsorption process describes the Freundlich equation, as indicated by the value of R^2, greater than 0.99. From Figure 4 it becomes clear that the value of the limiting adsorption (q_m) was not achieved during the experiment, and its value significantly exceeds 15 mg/g, which indicates an impressive sorption capacity of the sorbent under study. The maximum adsorption value obtained from the Langmuir equation, corresponding to 5.57 mg/g, does not correspond to reality - it is significantly underestimated, which indicates the inapplicability of the theory of monomolecular adsorption in the case with the sorbent chosen by us.

Thus, it was found that mercury adsorption on the PSTU-3F sorbent is the higher, the higher the acidity value, i.e. maximum sorption occurs in the strongly acidic pH range. This is due to the absolute dominance of the cationic form of the bivalent mercury Hg^{2+} and the negative charge of the surface of the sorbent. The increase in the mass of the sorbent has a significant effect on the shift of the pH of the solutions to a more alkaline region. The optimal ratio of the sorbent - solution should be considered the ratio of 1:1000. Freundlich's equation most accurately describes the process of mercury adsorption on the silicone sorbent PSTU-3F.

This work was supported by RFBR grant No. 17-05-01055.

References:

Voronkov M.G., Vlasova N.N., Pozhidaev Yu.N., Pestunovich A.E., Kirillov A.I. Highly effective complexitol and ampholyte - poly [N, N'- bis (silsesquioxanilpropyl) thiocarbamide] / / Reports of the Academy of Sciences of the USSR, 1991. Vol. 320, No. 3. P. 658–662. In Rus.

Vasilyeva I.E., Pozhidaev Yu.N., Vlasova N.N., Voronkov M.G., Filipchenko Yu.A. Sorption-atomic emission determination of gold, platinum and palladium in rocks and ores using PSTU-3F sorbent // Analytics and Control, 2010. Vol. 14. No. 1. P. 16−24. In Rus.

Nazarenko V.A., Antonovich V.P., Nevskaya E.M. Hydrolysis of metal ions in dilute solutions. M.: Atomizdat, 1979. - 192 p. In Rus.

Fiaizullina R.V., Makarova M.A., Abrosimova N.A. The possibility of wastewater treatment of heavy metals by natural sorbents // Proceedings of 17 international multidisciplinary scientific geoconference SGEM 2017. Vol. 52 of Soils, Forest ecosystems. STEF92 Sofia, Bulgaria, 2017. P. 1027–1034.

Karaseva O.N., Ivanova L.I., Lakshtanov L.Z. Modeling of strontium sorption on birnessite (δ-MnO_2) at elevated temperatures. UDC 550.4.02

IEM RAS, Chernogolovka, (olga@iem.ac.ru).

Abstract. Strontium sorption has been studied by the method of acid-base potentiometric titrations at three different temperatures: 25, 50, 75 ^{0}C. The effect of pH, ionic strength, sorbate/sorbent (Sr^{2+}/ ≡MnOH) ratio, and temperature on adsorption was investigated. Experimental data were simulated using the triple-layer model (*TLM*). The equilibrium model proposed here consists of the complexes of inner (>$MnOHSr^{2+}$, >$MnOSr^{+}$, >$MnOSrOH^0$) and outer types ([>MnO^-- Sr^{2+}]$^+$). The corresponding intrinsic equilibrium constants of the formation of these surface complexes were calculated for 25,50, and 75 °C.

Keywords: strontium; birnessite; sorption; surface complexation modeling; triple-layer model

In order to predict the migration of toxic substances and radionuclides in natural waters, study of the sorption interactions of strontium with manganese oxide have been carried out. Birnessite (δ-MnO_2) along with iron oxides is widely distributed in soils and sediments. The knowledge and consideration of the sorption mechanisms make it possible to create a thermodynamic model of the heterophase system, suitable for extrapolation in a wide range of concentrations, ionic strength and temperature.

Methods. The manganese dioxide was prepared by oxidizing $MnCl_2$ by slow addition of $KMnO_4$ (Balistrieri and Murray, 1982). The specific surface area of birnessite was determined by BET/Kr method to be 235 m^2/g.

Influence of pH, ionic strength, sorbate/sorbent (Sr^{2+}/ >MnOH) ratio, and temperature on adsorption were studied with the aid of experimental method representing a combination of potentiometric acid-base titrations and metal adsorption data. The equipment for titrations was described elsewhere (Karasyova, 1998,1999). The initial solid concentration in all experiments was 2 g L^{-1}.

This study was performed as a series of acid-base potentiometric titrations at 25, 50 and 75 ± 0.2 ^{0}C. The initial solid concentration in all experiments was 2 g L^{-1}.

Free proton concentration [H^+], i.e. proton concentration in the solution, was measured using the electromotive force of the cell (emf), for that the following equation is valid:

$$E = E_0 - 2.303\ RT/F\ p[H^+] + E_j, \qquad (1)$$

where E_0 is a constant determined for each experiment by acid-base titration of the background electrolyte solution. The liquid junction potential E_j, was found to be less than 0.1 mV within the experimental pH range and could be neglected in the calculation. The emf measurement was carried out with accuracy of 0.6 mVh^- (0.01 pH unit). Use of the concentration scale p[H^+] instead pH will be explained below.

A series of experiments was carried out to determine the total concentration of the surface sites, B_0, by titration of the birnessite surface by dilute NaOH solution. In this work, surface hydroxyl groups ≡MnOH formed on the mineral surface in contact with aqueous solution are considered as such surface sites. An excess of hydroxyls was evaluated from the data within the range 11< pH< 11.5 where the buffering effect of surface hydroxyl groups was found to be low, and could be corrected for in the calculations. Concentration of the hydroxyl groups could be determined by the difference between the total proton concentration H_{tot} and the free proton concentration [H^+]:

$$B_0 = H_{tot} - [H^+] + K_w / [H^+], \qquad (2)$$

where K_w is the ionic product of water. Calculation of the total proton concentration H_{tot} was performed as follows:

$$H_{tot} = \frac{(V_1 c_1 - V_2 c_2)}{(V_0 + V_1 + V_2)}$$, where V_0 is the initial volume of the suspension (mL), V_1 is the volume of added acid (mL), V_2 is the volume of added base (mL), c_1 and c_2 – acid and base concentrations (mol L^{-1}), respectively.

Strontium adsorption on birnessite surface has been investigated at various initial Sr concentration in the region 2 ≤ p[H^+] ≤ 12 at 25 and 75^0 C. Strontium solution of the known concentration was added to suspensions at p[H^+] ~ 2 - 2.5, and titration continued by diluted NaOH to p[H^+] ~ 12. Aliquots of the test suspension were sampled at known p[H^+] values and centrifuged. The total concentration of strontium in the aqueous phase was determined by Atomic Absorption Spectrometry.

Data treatment. Surface complexation models are widely and successfully used now to describe the surface-solution interactions. In this paper the adsorption equilibria are considered as the complexation reactions of strontium with the surface hydroxyl groups and can be written as:

$$p\ H^+ + q\ \equiv MnOH + r\ Sr^{2+} \Leftrightarrow [H_p(\equiv MnOH)_q Sr_r]^{(p+2r)};\quad \beta^{in}_{p,q,r}, \qquad (3)$$

for inner-sphere complexation, and

$$p\ H^+ + q\ \equiv MnOH + r\ Sr^{2+} \Leftrightarrow [(H_p(\equiv MnOH)_q]^p \ldots (Sr_r)]^{(p+2r)};\ \beta^{out}_{p,q,r}, \qquad (4)$$

for outer-sphere complexation, where *p, q* and *r* are stoichiometric coefficients.

Besides, it is necessary to take into account acid-base equilibria at the surface:

$$p\,H^+ + q{\equiv}MnOH^- \Leftrightarrow [H_p(\equiv MnOH)_q]^p \;;\; \beta_{p,q,0,} \qquad (5)$$

and the hydrolysis of Sr in aqueous solution:

$$p\,H^+ + r\,Sr^{2+} \Leftrightarrow H_pSr_r^{(p+2r)} \qquad \beta_{p,0,r,} \qquad (6)$$

$\beta^{in}_{p,q,r,}$,$\beta^{out}_{p,q,r}$, $\beta_{p,q,0}$ as defined by Equations (4-6) are apparent equilibrium constants which must be corrected for the electrostatic energy of the charged surface to obtain the corresponding intrinsic (int) constants:

$$\beta^{in}_{p,q,0}\,(int) = \beta^{in}_{p,q,0}\, e^{(pF\psi(0)/RT)}, \qquad (7)$$

$$\beta^{in}_{p,q,r}\,(int) = \beta^{in}_{p,q,r}\, e^{((p+2r)F\psi(0)/RT)}, \qquad (8)$$

$$\beta^{out}_{p,q,r}(int) = \beta^{out}_{p,q,r}\cdot e^{(pF\psi(0)/RT)}\cdot e^{((p+2r)F\psi(\beta)/RT)} \qquad (9),$$

where F is Faraday constant, R is the gas constant, T is the temperature (in K), $\Psi(0)$ is the electrostatic surface potential at the surface plane and $\Psi(\beta)$ is the potential at the β plane (for weakly bound ions).

There are various models of EDL for expression of interrelation between the surface charge and potential (Stumm, 1992). In this work, experimental data treatment was carried out using a Three-Layer Model of EDL which is applicable in the case of variable ionic strength and allows us to distinguish between specifically and non-specifically adsorbed ions. (Lützenkirchen, 1999).

The stoichiometric compositions and the corresponding equilibrium constants for the reactions at the birnessite – solution interface were evaluated with the aid of the computer program FITEQL 3.1 (Herbelin and Westall, 1994). The main indicator of goodness of fit is the overall variance $V(Y)$ which is the weighted sum of squares divided by the degrees of freedom. Values of $V(Y)$ between 0.1 and 20 indicate a reasonably good fit. Details on the optimization procedure have been described elsewhere (Karasyova et al., 1999; Herbelin and Westall, 1994). The distribution diagrams have also been calculated with the aid of the FITEQL program.

Results. Experimental data on the adsorption of H^+ and OH^-, obtained by potentiometric titration for two values of ionic strength, were used to estimate the constants of acid-base reactions using the TLM. The capacitance C_1 and the binding constants of the ions of the background electrolyte were fitting parameters (Herbelin and Westall, 1994) and varied to establish the minimum value of V (Y). Their values, as well as the values of the protonation and deprotonation constants are presented in Table 1. The used value of the capacitance of the outer layer (C_2) was 0.2 F / m^2 (Lyklema and Overbeek, 1961).

Table 1. Acid-base properties of the birnessite surface and Sr adsorption model calculated with the *TLM* at 25 and 75^0 C.

Reactions on the birnessite surface*		Results of calculations		
		25^0 C	*50^0 C*	*75^0 C*
$\equiv MnOH + H = \equiv MnOH_2^+$	$\beta^{in}_{1,1,0}$	2.82	2.50	2.03
$\equiv MnOH = \equiv MnO^- + H^+$	$\beta^{in}_{-1,1,0}$	-3.34	-2.5	-2.16
$\equiv MnOH + Na^+ = \equiv MnO^-\text{-}\,Na^+ + H^+$	β^{out}_{Na}	-3.0	-2.35	-2.19
$\equiv MnOH + H + Cl^- = \equiv MnOH_2^+\text{-}\,Cl^-$	β^{out}_{Cl}	2.82	2.90	2.59
$\equiv MnOH + Sr^{2+} = [\equiv MnOHSr]^{2+}$	$\beta^{in}_{0,1,1}$	-1.20	-1.70	-1.95
$\equiv MnOH + Sr^{2+} = [\equiv MnOSr]^+ + H^+$	$\beta^{in}_{-1,1,1}$	-5.85	-5.25	-4.4
$\equiv MnOH + Sr^{2+} + H_2O = [\equiv MnOSrOH]^0 + 2H^+$	$\beta^{in}_{-2,1,1}$	-12.53	-11.72	-10.6
$\equiv MnOH + Sr^{2+} = [\equiv MnO^-\text{-}\,Sr^{2+}]^+ + H^+$	$\beta^{out}_{-2,1,1}$	-1.07	-0.90	-0.6
Capacitance of inner layer** (F м$^{-2}$)		1.55	1.40	1.35
Goodness of fit *V(Y)*		15	12	19

* Density of surface hydroxyl groups is 6.4 sites/нм^2.
**C_2 was 0.2 F/m^2 based on the analysis of the compact-layer capacitance on AgI surfaces given by Lyklema and Overbeek [32]

Strontium adsorption on birnessite was studied as a function of pH, ionic strength, Sr total concentration, and temperature. The ratios of Sr(II) total concentrations and >MnOH were 0.1 and 1. Study of strontium adsorption was carried out in the range 2< pH < 12 at 25, 50 and 75 ^{0}C. As it can be seen in Fig. 1, strontium is strongly adsorbed to the birnessite surface within the investigated pH range for all temperatures. Adsorption of strontium on birnessite depends on ionic strength, especially, for low Sr concentrations.

Modeling of the system (>MnOH)-Sr^{2+}-H^+ with the help of the *TLM* consisted of the test of combinations of inner- and outer-sphere complexes with various stoichiometric compositions. The equilibrium constants for acid-base reactions and for electrolyte binding constants, surface site density, capacitances C_1 and C_2 (Table 1) were considered as known parameters and used without modification.

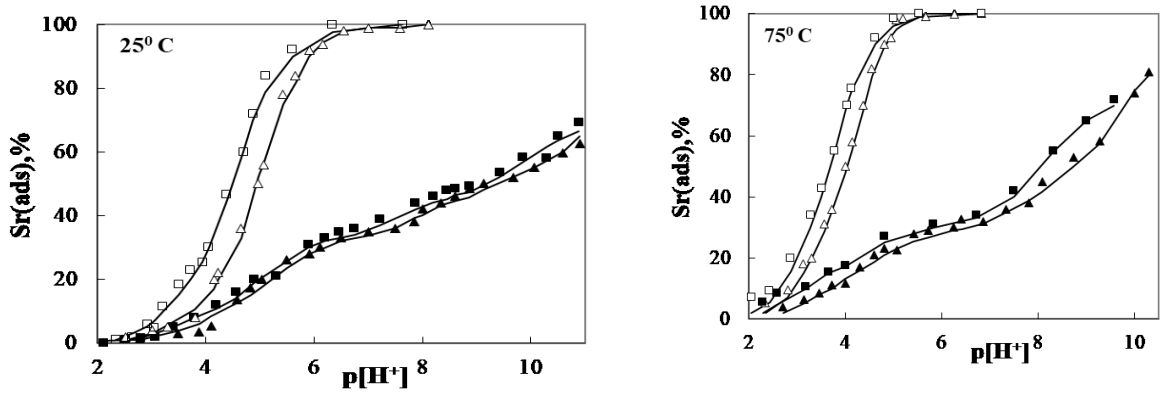

Fig. 1. pH dependence of Sr adsorption on birnessite (δ-MnO_2) at 25^0 C and 75^0 C. Intial $[\equiv MnOH]_{tot}$ = 5.0 mM. $[Sr]_{tot}$ /$[>MnOH]_{tot}$: 0,1 (□- 0,01 M NaCl; Δ - 0,1 M NaCl); 1,0 (■ - 0,01 M NaCl; ▲ - 0,1 M NaCl).

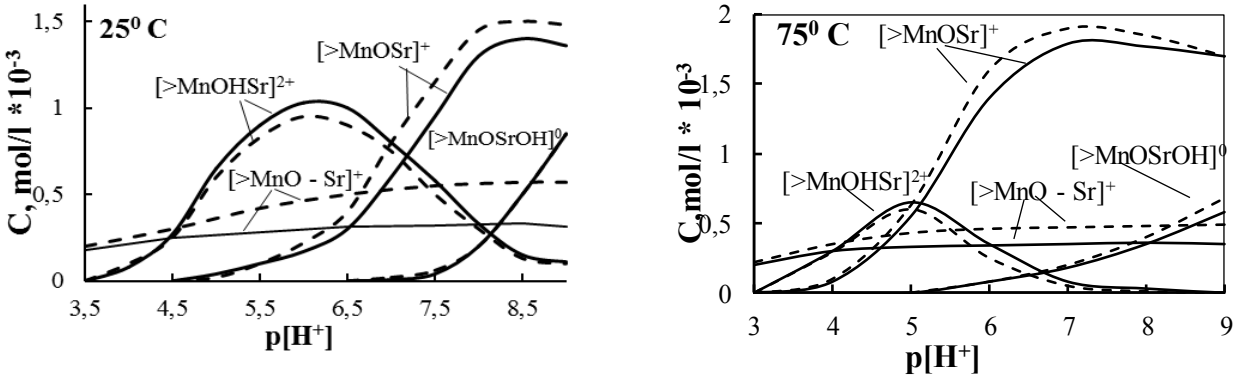

Fig.2. Distribution diagrams for surface complexes of Sr(II) at 25^0 C (a) and 75^0 C (b) calculated with using the *TLM*. $[Sr(II)]_{tot}/[\equiv MnOH]_{tot}$ ratio = 1.0. Solid curve shows the calculated values for complexes of Sr in 0.1 M NaCl, the dotted curves – in 0.01 M NaCl.

Reasonable good fit was obtained with only one model consisting of four complexes with overall stoichiometries defined according to Eq.4-5. These stoichiometries can be interpreted as a formation of three inner-sphere and one outer-sphere monodentate complexes. Any other combination of surface complexes of the more than 30 conceivable ones could not be optimized at all. Formation constants of the corresponding adsorption equilibria are given in Table 1. Fig.2 shows the distribution diagrams of Sr surface species under different conditions.

It can be noted that the concentration of the outer-sphere complexes on the birnessite is higher at low ionic strength and decreases considerably with increasing temperature. This behavior is characteristic of physical adsorption. The dominance of the inner-sphere Sr complexes at a higher pH can be explained by the increasingly negative surface charge on the birnessis due to the deprotonation of the surface groups and, consequently, their stronger attraction to positively charged Sr^{2+} ions from the solution. At high concentrations of Sr, the effect of ionic strength on adsorption is much weaker. With increasing temperature and Sr total concentration > $MnOSr^+$ becomes the dominant surface complex.

Conclusion. The results indicate that birnessite (δ-MnO_2) is of major importance in controlling Sr concentration in natural environments by direct adsorption. Sr adsorption is enhanced with decreasing ionic strength. This is probably due to a competing of Sr^{2+} ions with the electrolyte ions and, as a consequence, outer-sphere complexes along with inner-sphere complexes are formed. In this case, right the outer-sphere complexation is responsible for the total increasing the strontium adsorption.

The concentration of outer-sphere complexes is higher at low ionic strength and decreases with increasing temperature. The observed pattern is characteristic of physical adsorption. The dominance of the inner-sphere Sr complexes at a higher pH can be explained by the increasingly negative surface charge on the birnessite due to the deprotonation of the surface groups and, consequently, their stronger attraction to the positively charged Sr^{2+} ions from the solution.

References:

Balistrieri L.S. and Murray J.W. (1982) The surface chemistry of MnO2 in major ion seawater. *Geochim.Cosmochim.Acta* 46, 1041-1052.

Herbelin A.L. and Westall J.C. (1994) FITEQL: A computer program for determination of chemical equilibrium constants from experimental data, Version 3.1. Report 94-01. Dept. of Chemistry, Oregon State Univ. Corvallis, OR, USA.

Karasyova O.N., Ivanova L.I., Lakshtanov L.Z., Lövgren L. and Sjöberg S. (1998) Complexation of gold(III)-chloride at the surface of hematite. *Aquatic geochemistry* 4, 215-231.

Karasyova O.N., Ivanova L.I., Lakshtanov L.Z. and Lövgren L. (1999) Strontium sorption on hematite at elevated temperatures. *J. Colloid. Interface Sci*. 220, 419-428.

Lyklema J. and Overbeek J.Th.G. (1961) Electrochemistry of silver iodide the capacity of the double layer at the silver iodide-water interface. *J. Colloid. Interface Sci*. 16, 595-608.

Lützenkirchen J., (1999) The Constant Capacitance Model and Variable Ionic Strength: An Evaluation of Possible Applications and Applicability *J. Colloid. Interface Sci*. 217, 8-18.

Stumm W. (1992) Chemistry of the solid-water interface. New York: Wiley, 428 p.

Kotelnikov A.R.[1], Akhmedzhanova G.M.[1], Krinochkina O.K.[2] Composition of the surface water of shungite deposits study

UDC550.4.02, 553.9

[1]Institute of Experimental Mineralogy RAS (IEM RAS), Chernogolovka Moscow district, (kotelnik@iem.ac.ru);
[2]Moscow State University of civil engineering (MGSU), Moscow (vdovinaok@mail.ru)

Abstract. Sampling of surface waters at shungite deposits of Zaonezhie (Maksovskoye and Zazhoginskoe) were carried out. The solutions were analyzed for the content of major, minor, and impurity elements by the AAS and ICP-MS methods. It has been shown that the leading mechanism for converting heavy metals to soluble forms is the oxidation of sulfides (mainly pyrite) in near-surface conditions due to the increased oxygen potential and the presence of rainwater by the reaction: $FeS_2 + 2H_2O + 3O_2 \rightarrow Fe^{3+} + 2H_2SO_4$. The resulting acid contributes to the dissolution of ore sulphides (pentlandite, chalcopyrite, sphalerite, etc.), as well as rare earth phosphates, and the enrichment of natural waters with components such as rare earth elements, Co, Ni, Zn, Cd, Cu, etc. maximum permissible concentration (MPC) excess for elements such as Li (7); Be (3); Mg (2); Ti (5); Cr (4.5); Mn (63); Fe (460); Co (4.5); Ni (370); Cu (175); Zn (520); Cd (17.5); Tl (32); Pb (1.5); U (30) - the value in brackets is indicated (C_i/MPC). For the Zazhoginskoe deposit, the MPC excess was recorded only for the following elements: Mn (15); Fe (4); Ni (16); Zn (12). The development of the Zazhoginskoe deposit pollutes surface waters to a much lesser extent than the Maksovskoye development.

Keywords: shungite, surface water, deposits, rare earth elements.

Introduction

Despite the fact that shungites were studied by such eminent scientists as A.A. Inostrantsev, V.I. Kryzhanovsky, P.A. Borisov, L.Ya. Kharitonov, L.A. Bogdanov and many other and practical geologists (S. Kontrevich, N.I. Ryabov, M.M. Filippov, and others) during already the 2nd century, their genesis remains controversial. V.A. Melezhik et al. (Melezhik et al., 1999) for the first time introduced the concept of the "Shunga phenomenon". As early as 1879, the coal chemistry specialist K. Lysenko publishes information on two types of shunga "anthracite": "resinous black and shiny, with a shell-like fracture" and "dense, matt black."

Initially, shungites were considered as types of coal (Bogdanova, 2005), then – combustible shale, and later as vanadium ore (Filippov, Deines, 2018). Now shungite is widely used, it is used as a substitute for coke in the steel industry; in the production of ferroalloys; effective adsorbents for water treatment; catalysts for the organic synthesis of cyclic hydrocarbons, for the decomposition of hydrogen peroxide; active fillers for a wide class of composite materials with increased wear resistance, chemical resistance and electrical conductivity; radio shielding materials that protect people from man-made electromagnetic radiation; fertilizers that increase the yield and resistance of crops to diseases; feed additives to the food of fur animals, livestock and poultry. Some differences of shungite are promising as a source of raw materials for the currently developed technologies for producing aqueous dispersions of nanoparticles of modified carbon structure (Maximum Permissible Concentrations ..., 2000).

Currently, shungite is mined by the open method (Zazhogino and Maksovskoye deposits, Karelia.). During the development of shungite deposits, heavy metal production areas are contaminated. It is necessary to assess the extent of this process.

Methods and materials

Sampling was performed during the field seasons of 2016-2017. The waters (streams, small lakes, sewage collectors) of the Zazhogino and Maksovskoye shungite deposits were tested. For comparison, water was taken from Lake Onega (Tolvuya). Samples were studied by ICP-MS (IGEM RAS) and AAS (IEM RAS). Analyzes were carried out on the content of the main elements, ore and impurity (Table 1). In addition, the process of hydrolytic leaching of shungite was studied experimentally. For this, the shungite rocks of the Maksovo and Zazhogino quarries were crushed to a fraction of 1.4 - 2 mm. The average hitch for the experiments was 3 g. For leaching, we used: distilled water, 10% H_2O_2 solution, 10% sulfuric acid H_2SO_4 solution.

Table 1. The composition of the surface waters of the Maksovsky career.

Element	Ci, mg/dm^3	MPC, mg/dm^3	Element	Ci, mg/dm^{33}	MPC, mg/dm^3	Element	Ci, mg/dm^3	MPC, mg/dm^3
Li	0.215	0.03	As	0.048	0.05	Eu	0.272	-
Be	0.0006	0.0002	Rb	0.0074	0.1	Gd	1.082	-
Na	3.69	200	Sr	0.200	7	Tb	0.156	-
Mg	78.32	40	Y	0.043	-	Dy	0.694	-
K	21.1	50	Zr	0.051	-	Ho	0.119	-
Ca	43.72	180	Nb	0.0071	-	Er	0.309	-
Ti	0.47	0.1	Mo	0.072	0.25	Tm	0.033	-
V	0.079	0.1	Cd	0.874	0.05	Yb	0.2	-
Cr	0.446	0.1	In	0.0196	-	Lu	0.028	-
Mn	6.255	0.1	Cs	0.0004	-	Hf	0.0016	-
Fe	137.65	0.3	Ba	0.055	0.1	W	0.0033	0.05
Co	2.23	0.5	La	1.399	-	Au	0.0003	-
Ni	36.67	0.1	Ce	4.597	-	Tl	0.0032	0.0001
Cu	87.76	0.5	Pr	0.849	-	Pb	0.154	0.1
Zn	103.15	0.2	Nd	4.337	-	Th	0.0149	-
Ga	0.0045	-	Sm	1.17	-	U	1.481	0.05

The experiments were carried out in 100 ml teflon containers at two temperatures of 25 and 90°C. The temperature was maintained and controlled with an accuracy of ±1°C. The duration of the experiments was 60 days. Analysis of the solutions after the experiments was carried out using the AAS and ICP MS - AES methods. Then a correlation was made between the normalized values of the REE content in the quarry waters of the Maksovskoye deposit and experimental data on leaching from the same rocks.

Results and its discussion

It has been shown that the leading mechanism for converting heavy metals to soluble forms is the oxidation of sulfides (mainly pyrite) in near-surface conditions due to the increased oxygen potential and the presence of water by the reaction:

$$FeS_2 + 2H_2O + 3O_2 \rightarrow Fe^{3+} + 2H_2SO_4.$$

The resulting acid contributes to the dissolution of ore sulfides (pentlandite, chalcopyrite, sphalerite, etc.) as well as rare earth phosphates and the enrichment of natural waters with such components as rare earth elements, cobalt, nickel, zinc, cadmium, copper, etc. It is known that the sphalerite mineral contains significant quantities of rare elements – gallium and indium. When sphalerite is dissolved, they go into solution, which apparently also occurs in the surface waters of the Maksovskoye deposit, where the contents of copper, zinc and cadmium exceed the clarke levels several times. It is interesting to note that the content of such a rare element as indium reaches 0.01 mg/l and more than two times higher than the content of gallium (0.004 mg/ l). For the Maksovskoye deposit, the maximum permissible concentration has been established (Table 1) for elements such as Li (7); Be (3); Mg (2); Ti (5); Cr (4.5); Mn (63); Fe (460); Co (4.5); Ni (370); Cu (175); Zn (520); Cd (17.5); Tl (32); Pb (1.5); U (30) – the value in brackets is indicated (C_i/MPC). Hereinafter, the rationing was carried out with respect to the maximum permissible concentrations (MPC) of chemical substances in the water of water bodies of household, drinking, cultural and domestic water use.

Comparison of data on pollution of the surface waters of the Maksovskoye and Zazhoginskoye deposits allows to state that the development of the Zazhoginskoye deposit transforms surface waters to a much lesser extent than Maksovskoye, since the maximum permissible concentration for the latter was recorded only for the following elements: Mn (15); Fe (4); Ni (16); Zn (12).

In fig. 1 the normalized values of the REE content in the mine waters of the Maxsovskoye deposit with experiments on leaching of natural shungites is compared.

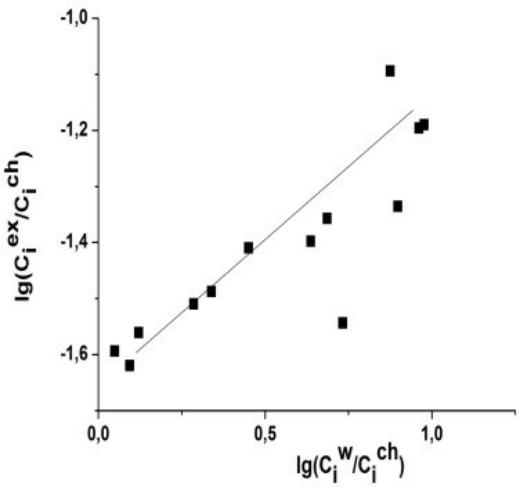

Fig. 1. Correlation of the normalized values of the REE content in the mine waters of Maksovo and in shungite leaching experiments.

Conclusions

1. Studied the composition of natural waters in areas of development of shungite deposits Zazhogino and Maksovskoye.

2. In the waters of the Maksovskoye deposit, an excess of the MPC has been established; for Li (7); Be (3); Mg (2); Ti (5); Cr (4.5); Mn (63); Fe (460); Co (4.5); Ni (370); Cu (175); Zn (520); Cd (17.5); Tl (32); Pb (1.5); U (30).

3. During the development of the Zazhoginskoye deposit, surface waters are polluted to a much lesser extent. Here the maximum permissible concentration is recorded only for the following elements: Mn (15); Fe (4); Ni (16); Zn (12).

4. Experiments carried out on modeling the processes of hydrolytic leaching of shungite substance showed the similarity of the experimental process with natural leaching.

References:

Bogdanova L.A. Transformation of coal in the zone of thermal effects of intrusions. Publ. VSEGEI. 2005. P. 15-17.

The maximum permissible concentration (MPC) of chemicals in the water of water bodies of drinking and household water use. Hygienic standards GN 2.1.5.1315-03, on the basis of the Regulation on State Sanitary-Epidemiological Regulation, approved by the Government of the Russian Federation dated July 24, 2000 N 554.

Filippov M.M. Shungite rocks of the Onega structure. Petrozavodsk: Karelian Science Center. 2002. 280 p.

Filippov M.M., Deines Yu.E. Sub-layer type of shungite deposits in Karelia. Petrozavodsk: Karelian Science Center. 2018. 261 p.

Melezhik V.A., Fallick A.E., Filippov M.M. et al. Karelian shungite – an indication of 2.0-Ga-old metamorphosed oil-shale and generation of petroleum: geology, lithology and geochemistry. Earth Science Reviews. 1999. V. 47. P. 1–40.

Kotelnikov A.R.[1], Akhmedzhanova G.M.[1], Krinochkina O.K.[2], Martynov K.V.[3], Kotelnikova Z.A.[4], Suk N.I.[1], Gavlina O.T.[5], Ananiev V.V.[6] **Experimental study of shungite of Zaonezhie** UDC 550.4.02, 553.9

[1]Institute of Experimental Mineralogy RAS (IEM RAS), Chernogolovka Moscow district, (kotelnik@iem.ac.ru; sukni@iem.ac.ru); [2]Moscow State University of civil engineering (MGSU), Moscow (vdovinaok@mail.ru); 3Frumkin A.N. Institute of Physical Chemistry and Electrochemistry RAS (IPCE RAS), Moscow; [4]Institute of Geology of Ore Deposits, Petrography, Mineralogy, and Geochemistry RAS (IGEM RAS), Moscow (kotelnik@igem.ac.ru); [5]M.V. Lomonosov Moscow State University, Chemical Faculty, Moscow; [6]Institute of Volcanology and Seismology (IVS RAS), Petropavlovsk-Kamchatskiy

Abstract. The study of minerals composition from shungite and host rocks of the Maksovskoye deposit (Zaonezhie, South Karelia) was carried out. Fluid inclusions in quartz from shungite and lidite host rocks were studied. On the basis of these data, the parameters of the mineragenesis of shungites of the Maksovskoye deposit are estimated. The leaching processes of the lithophylous, siderophylous, and chalcophilic elements of shungite have been experimentally studied. The effect of temperature, acidity of the environment, and oxygen potential on the hydrolytic stability of shungites is estimated. The correlation of the composition of shungite and the composition of the surface waters of the Maksovskoye deposit is shown. The sorption ability of shungite material was studied, the possibility of using shungites as a sorbent was evaluated.

Keywords: *shungite, fluid inclusions,* sorption capacity, leaching processes

The study of the composition of minerals from shungite and host rocks of the Maksovskoye deposit (Zaonezhie, South Karelia) and the study of fluid inclusions in quartz from shungite and lidite host rocks were carried out. On the basis of these data, the parameters of the mineral genesis of shungites of the Maksovskoye deposit are estimated.

Mineral thermometry. For the purposes of mineral thermometry, samples of carbonate-silicate rocks KT1021b (section Tolvuya-Tetyugino), KSH1013 and KSH1014 (Shunga) were selected. The studied rocks are dolomitized limestones with a large amount of silicate material. The study of minerals was produced by the microprobe method. The following minerals were found in the studied samples: dolomite, calcite, biotite, quartz, apatite, pyrite and rutile. Small amounts of iron and manganese are found in dolomite (up to 0.05 form units), calcite contains up to 2 mol.% of magnesite. In apatite, quartz and pyrite there are practically no impurities.

Apatite is essentially fluoride. Rutile contains impurities of vanadium (up to 3 wt.% V_2O_5), niobium (up to 9.5 wt.% Nb_2O_5), iron (up to 4.5 wt.% FeO) and uranium (up to 2 wt.% UO_2). Biotite is

actually fluorine-phlogopite. For mineral thermometry, coexisting calcite and dolomite are of interest. The occurrence of magnesium in calcite (in the presence of dolomite) is determined by the temperature of the mineral genesis. In the studied sample, the content of the magnesian minal in calcite varies from 0.5 to 1.9 mol.%. Recalculating the temperature of the mineral genesis (by calcite – dolomite thermometer) allows us to give the following temperatures: 350 ± 50°C. In shungite parageneses, phengite is present with an average composition of $K_{0.58}(Mg_{0.50}Fe_{0.10}Al_{1.58})(Al_{0.62}Si_{3.38})O_{10}[OH]_2$.

The Phe+Qz paragenesis can be used as a geobarometer (Kamzolkin et al., 2015). The pressure estimated by phengite compositions is 6±1 kbar. This pressure value is indirectly confirmed by the presence of single epidote crystals in the samples, which is stable at 350-400°C and P≥3.5-4.0 kbar. Chlorite of the composition $(Mg_{2.58}Fe_{2.14}Al_{1.22})_{5.94}(Al_{1.11}Si_{2.89})_{4.00}O_{10}(OH)_2$ (Maksovo) was found in the samples. The calculation by the chlorite thermometer (Cathelineau, Nieva, 1985) showed the value T=240 ± 10°C. Obviously, the peak of metamorphism was recorded by a calcite-dolomite thermometer and a phengite barometer (T=350°C, P= 6±1 kbar; and T=240°C, P=3.8 kbar), and chlorites and fluid inclusions recorded late stages of the process: T=240-150°C; P = 3.8 and P <0.5 kbar).

Study of fluid inclusions. For the study of fluid inclusions, quartz-containing samples were taken from carbon-containing rocks of the Tolvuya region. These were samples from Zazhoginsky career – KZ1002 (quartz and anthraxolite); from Maksovsky career – KM1005 (vein quartz) and the Tolvuya-Tetyugino section – KT1021a (silicified lidite). Microthermometric studies of fluid inclusions in quartz were carried out in all samples. It is shown that these inclusions are represented by types L and G + L. Temperature homogenization (in the liquid) vary in the range from 65 to 350°C. Salt concentration in fluid inclusions (NaCl-eq.) varies from 0.9 (sample KZ1002) to 10-16 wt.% (Sample KM1005 and KT1021a). The estimated fluid density ranges from 0.6 (sample KZ1002) to 0.92–0.96 (sample KM1005 and KT1021a). The study of fluid inclusions showed a relatively low temperature of their formation ~ 100-150°C, and the presence of syngenetic types of inclusions G + L and L indirectly indicates the formation of them from the layered fluid.

The composition of shungite rocks from Maksovsky career (Fig. 1) is presented in Table 1. It is seen that shungite rocks contain quite a lot of carbon matter – up to 45 wt.%. The silicate component is recalculated according to the CIPW method for regulatory minerals (Table 1). It is shown that it is represented, on average (in terms of 100%), by the following minerals: quartz (75.3%); feldspar (13.7%); corundum (4.2%); orthopyroxene (2.4%); hematite (2.2%); rutile (0.4%); apatite (0.3%); pyrite (1.4%).

Table 1. Compositions of shungite rocks of the Maksovsky career (Filippov and Deines, 2018) and carbonaceous matter.

Oxides	1	2	CIPW recalculation, %		
SiO_2	54.4	47.0		1	2
TiO2	0.23	0.25	Qz	47.93	41.25
Al_2O_3	3.74	4.16	Cd	2.10	2.77
Fe_2O_3	1.49	1.13	Ort	7.92	7.39
FeO	0.55	0.42	Ab	0.51	0.17
MnO	0.05	0.05	An	0.26	-
MgO	0.59	0.57	Hyp	1.47	1.42
CaO	0.17	0.08	Hem	1.50	1.13
Na_2O	0.06	0.02	Ru	0.23	0.26
K_2O	1.34	1.25	Ap	0.19	0.21
H_2O	0.8	0.7	Py	1.00	0.71
ппп	36.93	46.20			
P_2O_5	0.09	0.11			
Cr_2O_3	0.025	-			
V_2O_5	0.043	-			
Sum	99.57	99.62			
S_{tot}	0.90	0.38			
C_{opr}	36.6	44.6			

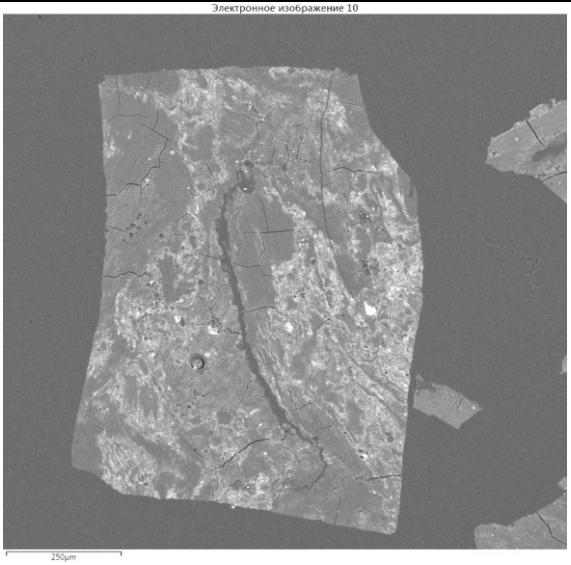

Fig. 1. Massive schungite rocks of the Maksovskoye deposite.

In the feldspar component, orthoclase dominates: Ort/Ab≈30. According to the ratio of modifying elements (Fe^{2+}+ Mn + Mg + Ca + Na + K) to the frame-forming elements (Si + Ti + Al + Fe^{3+}), shungites are close to metamorphosed quartzites. For shungites, this value is 0.057, for quartzites ~ 0.06. The composition of the carbonaceous component of shungite is as follows (wt.%): C – 82.42; O – 7.75; Na – 0.37: S – 0.37: Cl – 0.04; K – 0.07; V – 0.94; Fe – 0.04; Mo – 0.15. Attention is drawn to the significant concentrations of molybdenum and

vanadium — elements of biotic complexes. The Maksovsky shungites are enriched (relative to the clarks of the earth's crust) with the following elements: V (2.3); Cr (1.1); Ni (3.0); Cu (3.2); Zn (1.9); As (94); Mo (7.8); Cd (8.8); Sn (1.2); Au (11.7); Pb (1.6); U (3.8) – in parentheses the ratio of the element content in shungites to its clarke value (C_i^{Sh}/C_i^{Klk}) is indicated.

According to the spectra of normalized rare-earth elements (Sadovnichiy, 2016), shungites belong to essentially differentiated rocks: the ratio (La+Ce)/(Yb+Lu) in them is ~ 37; while for: granites – 32; syenite – 29; quartzite –24; clarks of the earth's crust – 23; N-MORB – 2.9; E-MORB – 8; chondrite C1 – 4.3.

The mineral composition of the massive shungites of the Maksovsky career is diverse. Among silicates and aluminosilicates, quartz, rutile, titanite, muscovite, potassium feldspar, phengite, epidote, allanite are encountered. Phosphates are represented by apatite and monazite. The most diverse ore minerals of the sulfide group are: pyrite, pyrrhotite, chalcopyrite, pentlandite, arsenic pyrite, sphalerite, lead sulfoselenide. Under the influence of meteoric waters saturated with oxygen, the oxidation of sulfides occurs, with the formation of sulfuric acid: $FeS_2+H_2O+3.5O_2=FeSO_4+H_2SO_4$.

Subsequently, the oxidation $Fe^{2+} \rightarrow Fe^{3+}$ happens and the mineral jarosite is precipitated from aqueous solutions: $K^+_{aq} + Fe^{3+}_{aq} + 2SO_4^{2-} \rightarrow KFe(SO_4)_2\downarrow$. Yellow friable masses of jarosite are found in almost all lakes and puddles of the Maksovsky career. At the same time, the acid acts on other sulfides, as a result of which elements such as Fe, Ni, Cu, Zn, Cd, Pb, As transfer to the aqueous phase. Also, minerals such as allanite and monazite containing rare earth elements are exposed to acids. Therefore, natural waters are enriched with REE. The compositions of surface waters are given in table 2. It can be seen that the contents of a number of elements (Li, Be, Mg, Ti, Cr, Mn, Fe, Co, Ni, Cu, Zn, Cd, Tl, Pb, U) in the surface waters of the Maksovsky career exceed the maximum permissible concentrations (Table 2).

The leaching processes of the lithophilic, siderophilic, and chalcophilic elements of shungite have been experimentally studied. The effect of temperature, acidity of the environment, and oxygen potential on the hydrolytic stability of shungites is estimated. The correlation of the composition of shungite and the composition of the surface waters of the Maksovskoye deposite is shown (Fig. 2).

The sorption capacity of shungite material was studied. The technique was as follows: shungite weighing 10 g (fraction 0.6-1 mm) was soaked in water in a glass column. The column had an internal diameter of 10 mm; the height of the layer of material in the column was 15 cm. When interacting with water, air was released from the material. In the water, the material was 3 days. Water was passed through a layer of shungite in the column. The outgoing volume of water was 50 ml. Then, 250 ml of 0.05N KCl solution was passed through a column with shungite and then washed with 50 ml of water to obtain the K-form exchanger. 250 ml of 0.05 N NH_4Cl was passed through the K-form in order to displace K+ from the exchanger and determine its ability to ion exchange and adsorption. Analysis of the solution obtained by the displacement of ammonium potassium ion, showed that the exchange capacity (including adsorption) of this sample is: 0.1 mg-eq. K = 0.0001 g-eq K = 0.0001 g-eq * 40 g/g-eq = 0.004 g. This is a very small sorption capacity.

Table 2. The composition of the surface waters of the Maksovsky career. MPC – maximum permissible concentration

Element	C_i	MPC	Element	C_i	MPC	Element	C_i	MPC
Li	0.215	0.03	As	0.048	0.05	Eu	0.272	-
Be	0.0006	0.0002	Rb	0.0074	0.1	Gd	1.082	-
Na	3.69	-	Sr	0.200	7	Tb	0.156	-
Mg	78.32	40	Y	0.043	-	Dy	0.694	-
K	21.1	50	Zr	0.051	-	Ho	0.119	-
Ca	43.72	180	Nb	0.0071	-	Er	0.309	-
Ti	0.47	0.1	Mo	0.072	0.25	Tm	0.033	-
V	0.079	0.1	Cd	0.874	0.05	Yb	0.2	-
Cr	0.446	0.1	In	0.0196	-	Lu	0.028	-
Mn	6.255	0.1	Cs	0.0004	-	Hf	0.0016	-
Fe	137.65	0.3	Ba	0.055	0.1	W	0.0033	0.05
Co	2.23	0.5	La	1.399	-	Au	0.0003	-
Ni	36.67	0.1	Ce	4.597	-	Tl	0.0032	0.0001
Cu	87.76	0.5	Pr	0.849	-	Pb	0.154	0.1
Zn	103.15	0.2	Nd	4.337	-	Th	0.0149	-
Ga	0.0045	-	Sm	1.170	-	U	1.481	0.05

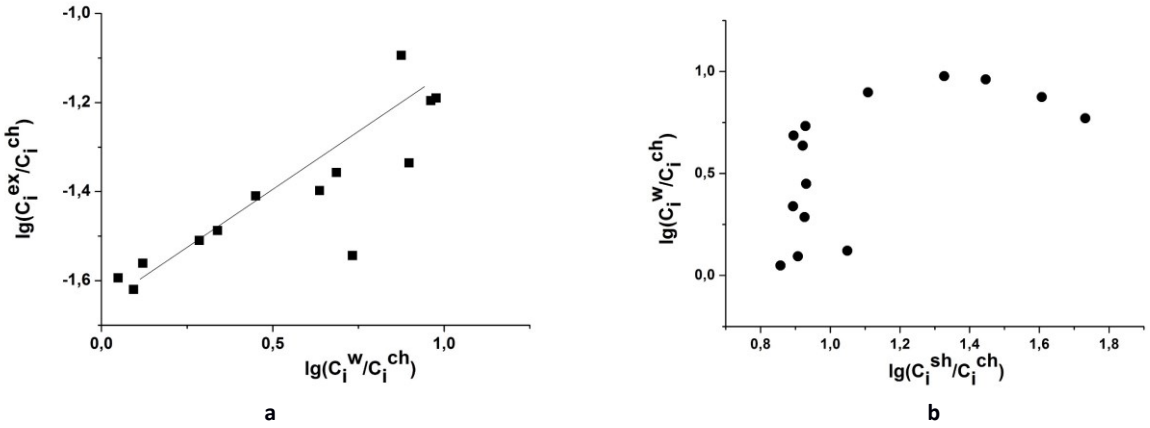

Fig. 2. Correlation of the normalized values of the REE contents in the pit waters of Maksovo and in leaching experiments (a) and comparison of the normalized values of the contents of REE in the pit waters of Maksovo with the normalized compositions of shungite (b).

Conclusions

1. The phase and chemical composition of shungite rocks of the Maksovsky career has been studied; high mineral diversity of mineral phases has been shown.

2. The composition of the natural waters of the Maksovsky career was studied, and the maximum permissible concentration for heavy metals, iron, manganese and uranium was shown.

3. Experiments were carried out on modeling the processes of hydrolytic leaching of shungite material. The similarity of the experimental process with natural leaching is shown.

4. Determined the sorption capacity of shungite substances. The sorption capacity of shungites is very low.

References:

Kamzolkin V.A., Ivanov S.D., Konilov A.N. Empirical phengite geobarometer: justification, calibration, application. Zapisky of Mineral. Society. 2015. Part 144. V. 5. P. 1-14.

Sadovnichiy R.V. Mineralogical and technological features of shungite rocks of the Maksovskoye deposit (Zazhoginskoe ore field). Dissert on Candidate of Geological and Mineralogical Sciences. Petrozavodsk. 2016. 137 p.

Filippov M.M., Deines Yu.E. Sub-layer type of shungite deposits in Karelia. Petrozavodsk: Karelian Science Center. 2018. 261 p.

Cathelineau M, Nieva D. A chlorite solid solution geothermometer The Los Azufres (Mexico) geothermal system. Contrib Mineral Petrol. 1985. V. 91. P. 235-244.

Kuleshova M.L.[1] and Danchenko N.N.[2] Experimental study of sand-gel material as a geochemical barrier for cadmium

[1] Department of Geology, Lomonosov MSU, Moscow, Russia, (Kuleshova rita5715@mail.ru) [2] V.V. Dokuchaev Soil Science Institute, Moscow, Russia

Abstract The laboratory study of adsorbing ability (N) of different types of sand-gel material (SGM) of undisturbed and remolded structure (with and without drying) in relation to cadmium was conducted in dynamic mode. The breakthrough curves were obtained and adsorbing abilities were calculated for different types of SGM, the comparative assessment of them was made. The contributions of poorly soluble hydroxide precipitation and adsorption itself to the total immobilization of cadmium were avaluated for each type of SGM. The effect of initial concentration of cadmium in solution and filtration velocity on adsorbing capacity was investigated. The results of study showed the perspectivity of SGM using as geochemical barrier in relation to cadmium.

Keywords: *aluminosilicate gels, sand-gel material, adsorption, cadmium.*

Introduction Artificial aluminosilicate gels, originally proposed for soil consolidation, have recently been increasingly considered as promising materials for the construction of protective geochemical barriers to the migration of dangerous inorganic pollutants into groundwater and surface water (Protection .., 1992; Savenko and Lapitsky, 2002; Samarin, 2015). Although in terms of sorption capacity for many metals, they are significantly inferior to activated carbon, zeolites, and many loamy soils (in particular, bentonites), due to a number of technological features of their use and economic affordability, aluminosilicate gels are a very attractive material for protective barriers.

Staging of the process of gelation and aging of the gel allows to obtain materials with different filtration and strength characteristics. Mechanical mixing of the gel with sand in the early stages of aging makes it possible to obtain not a solid mass, but a granular material with good filtration characteristics. Immobilization on SGM consists of the sum of two processes - the precipitation of poorly

soluble hydroxides and the sorption proper. When washing the gel, it is possible to gradually fill the entire intercellular space with distilled water or another non-alkaline solution without significant loss of gel strength (Voronkevich et al., 1978, Maximovich, 2012).

To make decisions about the feasibility of using the sand-gel screen at different sites that are sources of pollution, it is necessary to estimate its immobilizing ability against a wide range of hazardous pollutants. Earlier, we carried out laboratory studies of the absorptive capacity of SGMs of a damaged structure with respect to different radionuclides ions: Cs, Sr, Th, U, as well as Nd^{3+}- and VO_2^+- ions simulating actinides in oxidation states III and V. relation to most of the listed ions (Sergeev et al., 2009). The purpose of this work was to study the sorption capacity of SGM in relation to one of the most toxic elements – cadmium, occurring in the landfills filtrate, liquid waste of metallurgy, electroplating plants and a number of other industries in a concentration much higher than the MAC for waters of fishery facilities and for drinking one. The main objectives of the study were: 1) to compare the effectiveness of different types of SGM for cadmium removal; 2) to assess of the contribution of hydroxide precipitation and adsorption to the overall immobilization of cadmium; 3) to evaluate the influence of filtration velocity and the initial concentration of cadmium in solution on SGM adsorption capacity.

Materials and research methods Studies of the adsorption capacity were carried out on three types of SGM samples differed in filtration characteristics: 1) of undisturbed structure, 2) of impaired structure without drying, 3) of impaired structure with drying.

The aluminosilicate gel used in the experiments was prepared according to the described method [Lapitsky et al., 1992] by mixing a solution of sodium silicate and a complex hardener. The ratio of water glass and hardener was (1:0.7); gelation time - 0.5 h.

SGM was prepared on the base of preliminarily washed and dried sand.

SGM with undisturbed structure. The column with sand was placed into the prepared OAS sol, so that the sand was completely wetted with sol. After gelling the sample was used in experiments.

SGM with impaired structure. Sand was poured into the OAS sol, so that it was completely covered with sol and leave, after gelling completion the material was stirred thoroughly and, in one case, immediately placed into a column without drying (hydrogel), in the other - brought to an air-dry state (xerogel) and then placed in a column for further experiments.

Cadmium solutions. Aqueous solutions of cadmium sulfate with Cd concentrations 104 and 10.5 mg/l for samples of impaired structure, and 110 mg/l for a sample of undisturbed structure were used.

Experimental settings. The experiment for a sample with an undisturbed structure was conducted under the lapse rate J = 21.4 to shorten the experiment duration (K_f of this SGM = 0.00015 m/day). The filtration velocity (V_f) was 0.003–0.005 m/day. To assess the influence of high filtration velocity (≈1.0-3.0 m/day) on the immobilization ability of the SGM we carried out the experiment with the sample of impaired structure (without drying) under the lapse rate J=3.9. Filtration through the samples of impaired structure subjected to drying, was carried out at a constant velocity provided by Masterflex C/L peristaltic pumps, V_f ranged from 0.11 to 0.15 m/day for different experiments. Dynamic experiments were passed until the cadmium concentration in filtrate became equal to its initial concentration in solution supplied to the column. pH of each portion of the filtrate was measured immediately after collecting.

Cadmium concentrations in filtrate was determined by Hitachi Z-8000 atomic absorption spectrophotometer with flame atomization.

To assess the contributions of the precipitation and sorption processes to the total Cd immobilization by SGM, a parallel experiment was conducted on a dried sample of an impaired structure with preliminary washing out of the intermicellar liquid. Before filtering Cd solution, distilled water was passed through the column until the pH of the filtrate riched 7.5. Thus, this column gave the greatest possible immobilization by the sorption mechanism under these conditions. The contribution of the precipitation of poorly soluble hydroxide was evaluated with not washed samples.

Results and discussion *Evaluation of the adsorption capacity of SGM in relation to Cd in dynamic conditions.* Using the obtained values of Cd concentration in successive probes of the filtrate, we plotted the dependence of the relative concentration of cadmium in filtrate on the volume of solution filtered — breakthrough curves. Typical experimental breakthrough curves are given Fig. 1a-c by black lines.

Based on the processing of the breakthrough curves, the sorption capacity values (N_{Σ}.) of various types of SGMs with respect to cadmium were calculated. In a generalized form, the main parameters of the experiments and the results obtained are presented in Table 1. From a comparison of experimental breakthrough curves and calculated dependences of concentration of Cd ions in a solution on the volume of a filtered solution, it becomes apparent that at the initial stage of filtration Cd almost completely precipitates and the contribution of the hydroxide precipitation process to

the total immobilization of Cd is significant for all SGM samples not washed from intermicellar fluid.

As reflected by the data of Table 1, the SGM of the undisturbed structure (experiment 1) characterized with the lowest sorption capacity - 1.2 mg/cm^3. Apparently, this type of material has a denser structure and a smaller pore volume, which does not allow using all potential binding centers of sorbent. The N_{Σ} value of the hydrogel of the impaired structure (experiment 2) has a large value of 1.9 mg/cm^3, which is apparently due to the looser packing of aluminosilicate particles of this type of material and the larger area of the contacting surface of the sorbent with the solution. SGM of damaged structure with drying (xerogel) (experiment 3) offers the greatest immobilization ability - 2.2 mg/cm^3. This sample has an even looser structure, ensuring maximum contact of the Cd ions with the sorbent surface. It should be noted that in experiments with the same initial concentration of Cd (104 mg/l) and close filtration velocities (0.11 - 0.15 m/day) for all types of SGM of the impaired structure, obtained N values were very close (1.8 - 2.2 mg/cm^3).

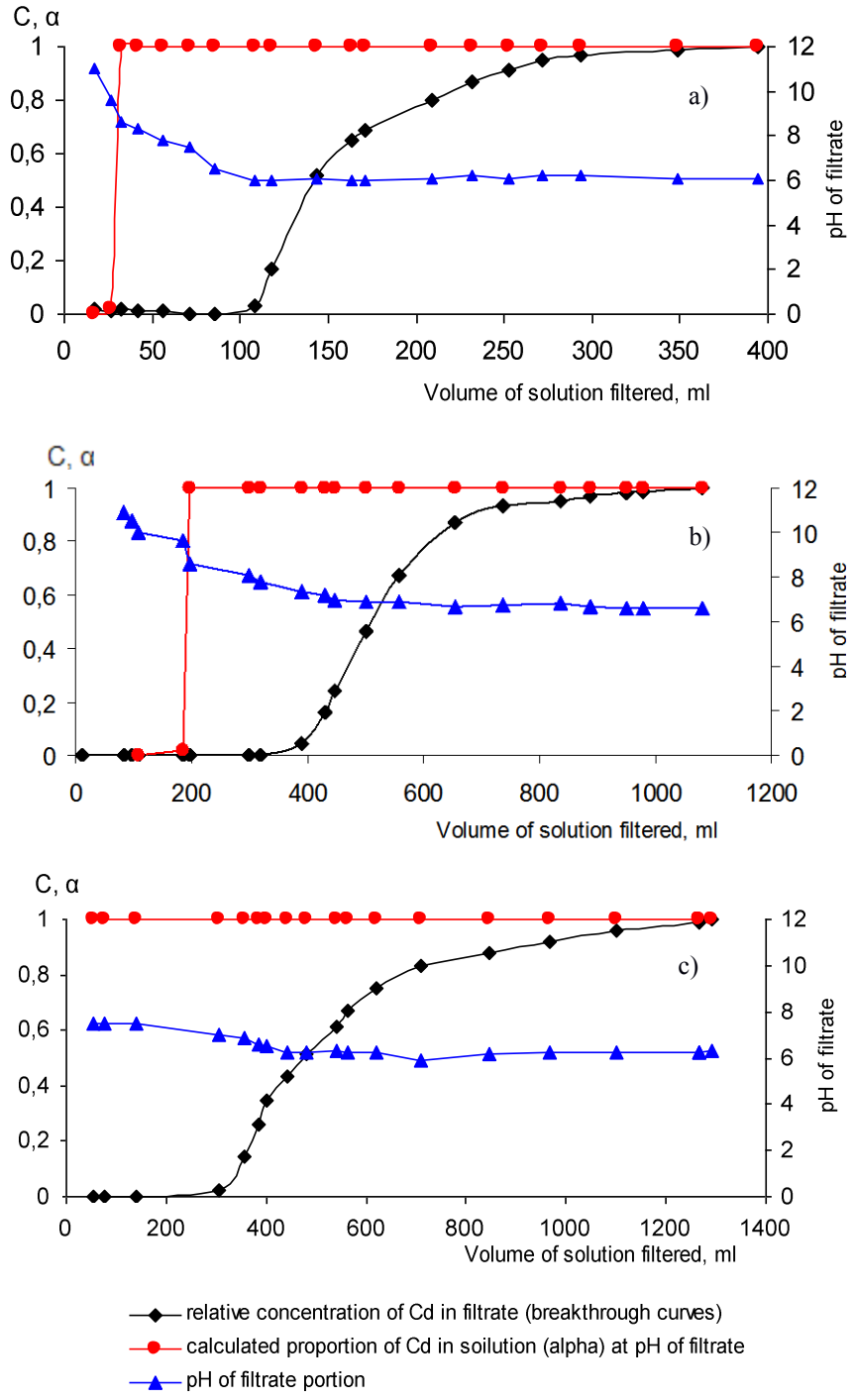

Fig. 1. Immobilization of cadmium by various types of SGM:

a) undisturbed structure, C_{Cd} = 110 mg/l; V_f = 0.004 m/day;

b) impaired structure without drying; C_{Cd} = 104 mg/l; V_f = 0.15 m/day;

c) impaired structure with drying and washing to pH 7.5; C_{Cd} = 104 mg/l; V_f = 1.11 m/day.

Table 1. The conditions and the results of studies of Cd immobilization by various types of SGM.

Exp. No.	SGM type	C_{Cd}, mg/l	V_f, m/day	Experiment duration, days	N_Σ, mg/cm^3	Contribution, % of precipitation	Contribution, % of sorption
1	undisturbed structure	110	0,004	363	1,2	19	81
2	hydrogel	104	0,15	10	1,9	37	63
3	xerogel	104	0,11	16	2,2	41	59
4	xerogel with washing to pH 7,5	104	0,11	15	1,8	-	100
5	xerogel	104	2,83	0,3	1,2	42	58
6	hydrogel	10,5	0,13	39	0,8	12	88

The effect of the initial concentration of cadmium in the solution on the N_Σ was estimated by comparing the results in experiments 2 (C_{Cd} - 104 mg/l) and 6 (C_{Cd} - 10.5 mg/l). While the difference in the initial Cd concentration is 10 times the adsorption capacity differs by 2.4 times (1.9 mg/cm^3 and 0.8 mg/cm^3). Filtration velocity V_f also affects the adsorption. An increase in the filtration velocity by 26 times (experiments 3 and 5, where V_f = 0.11 m/day and V_f = 2.83 m/day, respectively) lead to almost 2 times decrease in the adsorption from 2,2 mg/cm^3 to 1.2 mg/cm^3.

Contributions of precipitation and sorption to the total immobilization of Cd To determine the predominated Cd immobilization mechanisms at different stages, graphs of changes in the filtrate pH during the experiments (blue lines) are put together with breakthrough curves of various types of SGM. Using the tabular data of the solubility product (PR) of $Cd(OH)_2$ and the ionic product of water K_w by the formula:

$$\alpha = \frac{SP \cdot [H^+]^2}{C_{Cd} \cdot K_w^2}$$

, where *SP* - solubility product of $Cd(OH)_2$ = 2.21 10^{-14}; C_{Cd} - initial concentration of cadmium salt in the solution;$[H^+]$ - concentration of hydrogen ions in the solution;K_w - the ionic product of water; we calculate the proportion of cadmium ions in the solution (α) for pH values, corresponding to the pH of the filtrate, for solutions with two initial Cd concentrations: 9 10^{-4} mol/l and 9 10^{-5} mol/l used in the experiments. For clarity, the calculated relative concentrations of cadmium in a solution with the same pH as that of the filtrate, but in the absence of sorption, are also presented in Fig. 1 (red lines). Based on the calculated data, the amounts of Cd immobilized as hydroxide, were roughly estimated by integration of portions of the breakthrough curves from start to the pH above which more than 90% Cd presented as precipitate of hydroxide. It was pH 9.2 for experiments 1–3 and 5 (C_{Cd}≈100 mg/l), and pH 9.7 experiment 6 (C_{Cd} = 10.5 mg/l).

The share of cadmium precipitated as hydroxide for all SGM samples of the impaired structure was about 40% of the total quantity of immobilized Cd, and the proportion of sorbed - about 60% (see Table 1, experiments 2, 3, 5). For the undisturbed sample, the calculated contributions of these processes are approximately 20% and 80%, respectively (experiment 1). Obviously, in a sample with undisturbed structure, due to the low filtration rate, conditions are created for the partial dissolution of the formed precipitate during the passage of subsequent volumes of the solution with a more neutral pH. With a decrease in the initial concentration of the element in the filtering solution to 10.5 mg/l (test 6), the contribution of hydroxide precipitation to the total immobilization of cadmium is expected to decrease and is 10%.

In experiment 4 - SGM of impaired structure washed from intermicellar fluid - immobilization is associated only with sorption and amounted to 1.8 mg/cm. For a similar unwashed SGM sample (experiment 3), at the initial stage, the filtering solution interacts with a highly alkaline (pH≈11) intermicellar liquid and cadmium hydroxide precipitates. The estimated amount of cadmium immobilized due to precipitation in this experiment was 0.9 mg/cm^3, due to sorption 1.3 mg/cm^3. Thus, precipitation, on the one hand, increases the total immobilization of Cd, and on the other hand, prevents the achievement of maximum sorption. Filtration after the end of the precipitation period should obviously lead to a partial dissolution of the Cd hydroxide formed due to lowering the pH in the column, but the released Cd ions can be fixed by the sorption mechanism until the sorbent capacity is completely saturated. On this basis, it can be assumed that in the course of filtering water through the Cd-saturated sample, the amount of Cd that can be leached out is close to the difference between the total immobilization and the maximum sorption capacity of the washed material. To test this assumption, desorption experiments have begun.

Conclusions

SGM has a significant sorption capacity in relation to cadmium, which ranges from 1.2 to 2.2 mg/cm^3, depending on the structural characteristics of the material. This allows us to recommend it as a material for an anti-migration sorption screen.

– Two processes contribute to the total immobilization of cadmium on SGM:

precipitation in the form of hydroxide and sorption. The shares of these processes depend on the characteristics of the material and the concentration of the element in the filtering solution. For varieties of SGM with impaired structure and cadmium concentration of about 100 mg/l, they were 40% and 60%, respectively. Lowering the initial concentration of cadmium to 10 mg/l decreases the precipitation share to 10%.

- The sorption capacity of SGM depends on the concentration of cadmium in the initial solution - a reducing concentration by 10 times (from 104 mg/l to 10.5 mg/l) leads to a decrease in the magnitude of sorption by 2 times.
- The velocity of solution filtration through the layer of SGM also affects the absorption of Cd: increasing the velocity from 0.11 to 2.8 m/day (25 times) reduces cadmium immobilization by almost 2 times (from 2.2 to 1.2 mg/cm^3).

References :

Danchenko N. N. et al. 2011. Study of the properties of artificial composite materials for permeable geochemical barriers //Moscow University Geology Bulletin. v. 66. No. 5. p. 354-360.

Maksimovich N. G. 2012. Changes in the properties of silicate grouting materials used in the technical melioration of soils. // Engineering geology. No. 4. P. 14-24. (in Russian).

Polevich O. V., Udalov I. V., Chuenko A. V. 2017. The use of special geochemical barriers to block the spread of heavy metals and radionuclides by underground man-made streams. Problems of Atomic science and technology. Series: Physics of Nuclear Reactors. V. 108. No. 2. P. 194–200 (in Russian).

Protection of groundwater from pollution in the areas of designed and existing tailings. 1992. (Ed. Sergeev V. I.) Publishing House of Moscow State University. Moscow. 168 pp. (in Russian).

Savenko A. V., Lapitsky S. A. 2002. Prospects for the use of geochemical barriers based on aluminosilicate gels to protect groundwater from pollution, Proc. International scientific methodological conf. “Ecology - education, science and industry”. Vol. 2. Belgorod. P. 116–124. (in Russian).

Samarin E. N. 2015. On the issue of classification of injection materials. // Geotechnics. No. 4. P. 52–61

Samarin E. N., Rodkina I. A., Kravchenko N. S. 2018. Toxicity of injection materials used in soil reclamation. // Ecology and Industry of Russia. Vol. 22. No. 10. P. 66-71. (in Russian).

Sergeev V. I., Danchenko N. N., Kuleshova M. L. et al. 2009. Evaluation of the effectiveness of sand-gel material as a sorption screen on the path of migration of radionuclides // Problems of Atomic Science and Technology. Series: Physics of Nuclear Reactors. No. 1. p. 42–48. (in Russian).

Voronkevich S. D., Evdokimova L. A., Sergeev V. I. 1978. Theoretical foundations and results of the introduction of methods of chemical plugging of semi-rock and rock rocks // In the collection: Problems of engineering geology and soil science. Vol. 4. Publishing House of Moscow State University. Moscow. P. 199–209. (in Russian).

Makarov V.P. On the mechanism of weathering of orthoclase in the oil terrigena the Fergana depression. UDC 551.311.22+553.2

Russian State Geological Prospecting University, Moscow, Russia (litology-kaf@mgri-rggru.ru)

The results of [Akramkhodzhaev, 1960] of studying the Cretaceous sediments of the Fergana Valley are examined in order to identify new features of the formation of mechanogenic, especially sand, reservoirs based on the use of new materials interpretation techniques. Research covered areas of Uzbekistan and Kyrgyzstan. Studied are the strata and components of their formations, composed in various combinations of sandstones, sandy-clay and clayey formations, siltstones, conglomerates with gravelites, carbonates, sometimes with dolomites, sulfates.

All samples were subjected to petrographic and mineralogical studies in thin sections and immersion preparations. In the loose samples, the "light" and "heavy" fractions in samples of 0.10-0.01 mm in size were distinguished. The following were established: the light fraction — the main minerals: quartz Qw, feldspars (potassium spars Kf — orthoclase and microcline, rarely plagioclase Pl), fragments of clay aggregates (HA); rare minerals and accessories: biotite, muscovite, mica (without separation), dolomite, kaolinite Kao, etc. The heavy fraction is the main minerals: magnetite Mt + ilmenite Il, hematite + limonite, garnet, zircon, tourmaline; rare minerals: stavrolite Stavr, sphene, epidote, chlorite, barite; accessories: celestine, biotite, muscovite, amphiboles, etc. The basic techniques for studying minerals are the construction of correlation straight lines of the Y = AX + B type, the calculations of their parameters and the construction of compensatory lines B = (Xo) A + Bo if necessary [Makarov, 2006]. The important point is to clarify the physical meaning of the parameters of these equations. In order to describe the mechanisms of the relationship of minerals applied thermodynamic analysis. Direct observations have shown that HA fragments are mainly composed of clay-sericite formations and montmorillonite, beidelite, hydromica (hydrobiotite and hydromuscovite [illite]) and kaolinite are installed in them, but quantitative ratios between the clay minerals are not given.

The analysis revealed that, firstly, in approximately 95% of the samples between the mineral content, the correlation is completely absent; in the diagrams, points form a cloud of indefinite

form without an internal structure in their distribution. Further, such structures will be called "cloud" (Fig. 1A). Direct observations have shown that HA fragments are mainly composed of clay-sericite formations and montmorillonite, beidelite, hydromica (hydrobiotite and hydromuscovite [illite]) and kaolinite are installed in them, but quantitative ratios between the clay minerals are not given.

Secondly, internal structures appear much less frequently in this cloud: both a linear relationship and a cloud distribution are revealed. Planned geographical differentiation of matter. The same situation is observed in the Muyakan Formation and sub-empathic thicker, but spatial differentiation in them is already absent. Thirdly, in very rare cases, a linear relationship is established (Fig. 1B) between the mineral content. First of all, this is typical of the pair "potassium feldspar-clay aggregates" (9 samples) (Fig. 1B). All of them evon written in table.1. In the compensation diagram [Makarov, 2006], the points are grouped along the straight line A = -43.82B + 23.68 (Fig. 1B). It can be assumed that the composition of the source of these minerals is approximately constant and corresponds to the initial concentrations of potassium feldspar (Kf) o = 43.82% and clay aggregates (HA) o = 23.68%. In addition to this pair, Kf - Pl (Pl =0.009Kf +0.059), (Mt + Il) - Stavr [Stavr = 0.187 (Mt + Il) - 3.005], (Mt + Il) - Tur [Tur = 0.107 (Mt + Il)], and also the relationship Kf = 0.352 Qw + 9.003 and Kf = 0.715Qw + 0.26.

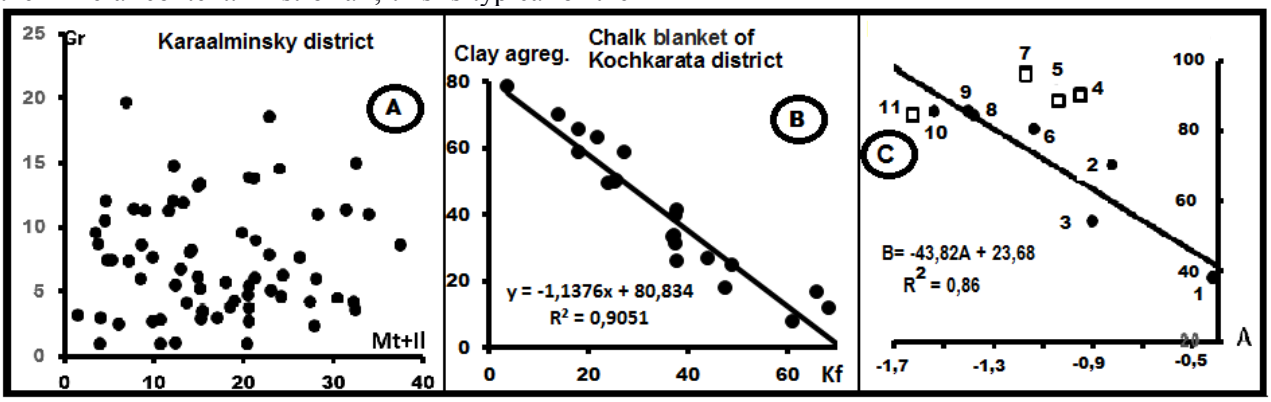

Fig.1. Types of connections between minerals. A-cloud and B-linear distribution between minerals; C-compensation equation.

Table 1. The parameters of the equation Kf = A (CA) + B between Kalishpat (Kf) and clay aggregates. (CA)

№№ p.p.	Districts	A	B	R^2
1	Varzyk	-0,423	37,82	0,984
2	Gulchinsky	-0,826	70,34	0,918
3	Tokubai	-0,903	54,39	0,540
4	Varzyk	-0,954	90,39	0,994
5	Lyakanskaya Retinue	-1,040	88,04	0,888
6	Kochkaratinsky	-1,137	80,83	0,905
7	Muyan Formation	-1,171	96,44	0,908
8	Karaalminsky	-1,379	84,48	0,901
9	Changyrtash-Suzaksky	-1,398	85,65	0,958
10	Abshirsky	-1,539	85,56	0,902
11	Naukatskiy	-1,625	84,70	0,875
12	Naryn	-5,215	87,05	0,827

Thus, patterns are highlighted:

1. The sequence in the formation of a correlation connection:

a) cloud distribution - the predominant type of distribution (Fig. 1A);

b) mixed distribution - a combination of cloud and linear distribution; c) linear distribution-relationships are described by equations of the form M1 = cM2 + C. In the overwhelming majority of cases, R^2 >> 0.80 (Fig. 1B). The nature of the distribution over the area of these types of communication could not be established. Nevertheless, it can be assumed that the distributions of the third type are initial, and later, under the influence of various processes of rock transformation, this distribution was destroyed, the mineral components of the sample were mixed, creating, eventually, a uniform "cloudy" distribution.

2. The distribution of the form (CA) = AKf + B (A <0) for the minerals Kf and HA is the original. "... in some cases, an increase in the number of clayey small-scaly formations is associated with a decrease in the number of feldspars and, vice versa ..." [Akramhodzhaev, 1960, p. 203]. Since A <0, we can say that these conclusions confirm the observations of A.M. Akramkhodjaeva. However, he did not consider the mechanism of such a separation.

Taking into account the sign with constant A, this equation is considered as the sum of two components, which is a constant quantity, i.e. we have (HA) + AKf = B = const. Here one component is replaced by another component. This is a typical manifestation of the process of mixing the components, but there can be several mixing mechanisms: mechanical entry of one of the components into the mixing zone; mixing takes place due to a chemical reaction, as a result of which one of the components disappears and the other appears; for example, by reaction [Koronovsky, 2018]:

$2KAlSi_3O_8 + 2H_2O + CO_2 \rightarrow H_2Al_2Si_2O_8 \cdot H_2O$ *) + $+ K_2CO_3 + 4SiO_2$. (1)

These equations reflect the direct transition of orthoclase to a mixture containing kaolinite. In detail, the existence of this phenomenon in natural conditions, no one checked. Analysis (1) for the conditions of thermodynamic equilibrium shows the following: a) Since this reaction is a substitution reaction, Kf and Kao should be in inverse relationship: a decrease in Kf should be accompanied by an increase in the Kao content, and vice versa. The same can be said about the relationship between Kf and quartz Qw; b) Since the number of particles involved in the reaction is not equal in both parts, the reaction depends on the pressure, and as the external pressure increases, it shifts to the left, i.e. Kao is not formed; c) To assess the effect of T on the course of the reaction, the values of **Δ**G for standard conditions (T = 298°K and P = 1 atm.) and T = 373°K (according to the approximate equation $\Delta GrT \approx \Delta H^o_{298} - T \cdot \Delta S^o_{298}$ [Dukhanin, 2010]) are determined. The initial thermodynamic data are given in table 2. Then in the first case, ΔG^o_{298} = 19.36 kcal / M, in the second case - ΔG^o_{373} = 24.18 kcal / M. In both cases, the values of the Gibbs free energy are positive, saying that the reaction is always shifted to the left. Therefore, Kao is not formed directly by the decomposition of Kf.

3. On the other hand, with an excess of completely mobile components H_2O and CO_2 on the left side of the equation, and also when you remove the right side of the potash and quartz as the reaction proceeds, the reaction tends to move to the left, i.e. towards Kao education; but here dynamic factors appear, corresponding to non-equilibrium thermodynamic conditions. Observations have shown that when free Kao is present in the rocks, Kf - Kao points form a cloudy distribution, i.e. there is no connection between minerals. And, therefore, the feedback (Kf - GA) is not due to the reaction between Kf and Kao. This assumption is also supported by the absence of a connection or a direct connection between Kf and Qw.

In the literature [Chertko, 2007], the reaction $2KAlSi_3O_8 + 3H_2O = 2KOH + H_2Al_2Si_2O_8 \bullet H_2O + 4SiO_2$, which occurs in the presence of CO_2, is also mentioned; it is generally close to reaction (1). For this equation, ΔG^o_{298} = 225.6 kcal / M, this value is positive and so great compared with previous estimates of **Δ**G, which indicates a low probability of it in general. In addition, this statement is contradictory: according to [Chertko, 2007], "kaolinite is stable in a strongly acidic and acidic environment," here a strong alkali is established in the right-hand part, which does not correspond to this condition.

Table 2. Initial thermodynamic data [Karpov, 1968].

Compounds	$-\Delta H^o_{298}$, Ccal/M	$-\Delta G^o_{298}$, Ccal/M	ΔS^o_{298}, Cal/M·K	$c_p = a + bT + c/T^2$		
				a	$b \cdot 10^3$	$c \cdot 10^{-5}$
$KAlSi_3O_8$ (ortoclase)	946,10	892,7	50,7	63,83	2,90	-17,05
H_2O (liquid)	68,31	56,69	16,716	18,08	-	-
CO_2 (gas)	94,05	94,26	51,061	10,57	2,10	-2,06
Kaolinite	978,1	901,4	48,5	57,47	35,3	-7,87
K_2CO_3 (solid)	273,93	255,5	33,7	19,19	26,06	-
SiO_2	217,65	204,64	9,88	11,22	8,20	-2,7
Muskovite (sericite) $KAl_2(Al_3O_{10})(OH)_2$	1424,4	1334,2	70,82	97,56	26,38	-25,44
KOH (solid)	101,78	89,5	14,2	No dates		

V.T. Frolov [Frolov, 1992] gives the equation for the decomposition of Kf with the formation of sericite:

$6KAlSi_3O_8 + 2H_2O + 2CO_2 = 2KAl_2 (Al_3O_{10}) (OH)_2 + 2K_2CO_3 + 12SiO_2$.

For muscovite (sericite) (Table 2) ΔG^o_{298} = 22.97 kcal / M, i.e. under standard conditions, this reaction should proceed in the direction of preserving Kf. Since for the reaction $\Delta S^o_{298} > 0$, it will be shifted to the left and with an increased T.

Many authors [Gorshkov, 1973] propose a phased mechanism for the transformation of Kf into Kao. At the first stage, intermediate minerals of the type of montmorillonite, hydromica or sericite are formed (no relationships have been established), at the second stage they turn into Kao. The data

obtained suggest that all micaceous minerals, including montmorillonite, cannot directly replace Kf. First of all, this discrepancy to realities may be because the above equations do not reflect true connections between minerals, and therefore do not allow adequately describing the relationship between Kf and Kao. The paper [Weathering ...] mentions the connection of the Kalishpat with hydromica (illite) $K[AlSi_3O_8] \rightarrow (K,H_3O)Al_2(OH)_2[AlSi_3O_{10}]$ (illite) $\rightarrow Al_4(OH)_8[Si_4O_{10}]$, but the reaction itself is not spelled out

Thus, in the process of rock formation, the relationship between Kf and Kao is influenced mainly by the mixing of minerals from a certain source. The composition of this source is determined by the values of the contents of minerals: Kalishpat $(Kf)_o = 43.82\%$ and clay aggregates $(CA)_o = 23.68\%$

*) Note: Kf has two forms of writing; in the above equations, it is written as $H_2Al_2Si_2O_8 \cdot H_2O$, and in [Karpov, 1968] - as $Al_2Si_2O_5(OH)_4$. Thermodynamic data from table 2 refer to the second form. The identity of these equations is not clear. Although the set of elements and their quantities are the same in both records, but their structural position is different, which means that they must have different thermodynamic parameters. In addition, the form $Al_4[Si_4O_{10}](OH)_8$ [Weathering ...], which is a double version of the second species, is also mentioned. And here their thermodynamic identity is not clear.

References:

Akramkhodjaev A.M. Lithology of oil and gas deposits of the Fergana Depression. Tashkent: Publishing House of the Academy of Sciences of the Uzbek SSR, 1960.

Weathering (hypergenesis) of rocks. URL: http://Roznayka.org/s102863t1.html.

Gorshkov G.P., Yakusheva A.F. General geology. M .: MSU edition, 1973. 592

Dukhanin G.P., Kozlovtsev V.A. Thermodynamic calculations of chemical reactions. Volgograd: Volg-GTU, 2010. URL: https://www.twirpx.com/file/490490/

Karpov I.K., Kashik S.A., Pampura V.D. Constants of substances for thermodynamic calculations in geochemistry and petrology. M .: Science, 1968

Koronovskiy N.V. General geology. M .: KDU "DOBROSVET", 2018.

URL: https://bookonlime.ru/product/obshchaya-geologiya

Makarov V.P. “Compensation Phenomenon” - a new type of connection between geological objects. / Materials of the I International. scientific and practical conference "The formation of modern science - 2006". Dnepropetrovsk, 2006. Vol.10, pp. 85-115. URL: http://www.lithology.ru/node/817

Rukhin L.B., Rukhina E.V. Cretaceous sediments of the Fergana basin. L .: Publishing House of Leningrad State University, 1961.

Frolov V.T. Lithology. Book 1. M .: Publishing House of Moscow State University, 1992.

URL: http://docplayer.ru/29098236-V-t-frolov-litologiya-kniga-i.html#show_full_text/.

Chertko N.K. Geochemistry. Minsk, TETRA SYSTEMS Publishing House, 2007. URL: http://elib.bsu.by/bitstream/123456789/24189/1/geochem07.pdf.

Zharikov A.V.[1], Malkovsky V.I.[1,2] A new method of experimental study of rock sample permeability UDC 552.08

[1]*Institute of Geology of Ore Deposits, Petrography, Mineralogy, and Geochemistry, Moscow,* [2]D.I.Mendeleev University of Chemical Technology of Russia, Moscow

Abstract Experimental studies of rock permeability for aqueous fluid in the near-critical domain of state are associated with significant difficulties. In this regard, it is proposed to use carbon dioxide in experiments for filtration through a sample instead of water, because CO_2 is thermodynamically similar to water, and the dependences of its thermophysical properties on the given parameters almost exactly correspond to the same ones for water. At the same time the critical parameters of CO_2 are significantly lower than those of H_2O. Therefore, using the thermodynamic similarity of these two fluids, it is possible to estimate the nature of changes in the permeability of rocks in the supercritical and near-critical domains of H_2O. The theoretical basis of the technique and the scheme of the experimental setup are developed.

Keywords: *rock sample, permeability, fluid, supercritical parameters*

Rock permeability which is one of the main parameters responsible for the dynamics of fluid heat and mass transfer in the deep zones of the Earth's crust, significantly depends on the fluid properties. Hence, it can be expected that its character for aqueous fluids in the supercritical and especially in the near-critical region of the state parameters will differ significantly from that determined in experiments on a weakly compressible liquid or gas, in properties close to ideal, as is currently accepted [Shmonov et al., 2002; Malkovsky et al., 2013]. However, experimental studies of rock permeability for aqueous fluid in the near-critical region are associated with significant difficulties. In this regard, it is proposed to use carbon dioxide, which is thermodynamically similar to water, in experiments for filtration through a sample instead of water, i.e. the dependence of its thermophysical properties on the above state parameters almost exactly correspond to the same dependencies for water. However, the critical parameters of CO_2 are significantly lower than those of H_2O. Therefore, using the thermodynamic similarity of these two fluids, it is possible to estimate the nature of changes in the permeability of rocks in the supercritical and near-critical area of H_2O. The theoretical basis of the technique and scheme of the experimental setup, which for the first time will determine the permeability of rock samples in the filtration of

carbon dioxide at near-critical parameters are developed.

A concept of the new method of permeability determination using for filtration CO_2 as thermodynamical analogue of H_2O fluid.

For various geological applications, it is necessary to determine the rock transport properties for aqueous fluid at near - or supercritical values of *PT*-parameters. In this case, the characteristics of the filtration process can be significantly influenced not only by the dependence of the rock permeability on the temperature for a homogeneous fluid, but also by the strong variability of its thermophysical properties near the critical point. Due to the relatively high values of the critical temperature (T_{cr}) and the critical pressure (p_{cr}) for an aqueous fluid, experimental determination of the rock permeability for the fluid in the near-critical domain of its state parameters is a matter of substantial difficulty. That is why it seems to be worthwhile to carry out the experiments on modeling liquids [Miropolsky, Soziev, 1990]. Substances are thermodynamically similar to each other for certain parameters (e.g. for density and dynamic viscosity) if ratio of corresponding parameters of the both substances at the same values of reduced pressure $\pi = p / p_{cr}$ and reduced temperature $\tau = T / T_{cr}$ are close to constant values. It is obvious that process of fluid filtration in a porous medium depends on the dynamic viscosity of the fluid. Taking into account the Klinkenberg effect, one can expect that the fluid density exerts also an influence on the filtration nature. Therefore, it is reasonable to select such modeling substances for the experiment which are thermodynamically similar to H_2O from the viewpoint of density and dynamic viscosity. Carbon dioxide can be considered as such modeling substance. The critical values of pressure and temperature for H_2O and CO_2 are presented in Table 1. Therefore, if water and carbon dioxide are thermodynamically similar in density and dynamic viscosity, the experiment for the same values π and τ at $\tau \geq 1$ can be carried out on CO_2 and it seems much simpler than on H_2O.

Table 1. Critical parameters of H_2O and CO_2

Substance	p_{cr}, MPa	T_{cr}, K
H_2O	22.1	647.2
CO_2	7.38	304.2

Plots of density and dynamic viscosity against reduced pressure and reduced temperature for water and carbon dioxide from [Miropolsky, Soziev, 1990] are presented below in Fig. 1–3.

For such purpose, the gas-cylinder in operation state is mounted so that its valve is at the bottom. We denote volumes of the thermal press and the receiver as V_0 and V_1, respectively. Then the valves in front of the thermal press and behind the receiver are closed. As a result of electric heating temperature in the thermal press increases up to $T_1 > T_0$. Due to thermal expansion of CO_2 in the thermal press, the pressure increases in the thermal press and in the receiver, as well, up to a value p_c. This value is controlled by variation of T_1 due to adjustment of electric heating of CO_2 in the volume of the thermal press. As the value of p_c reaches a prescribed value, the valve between the thermal press and the receiver is closed, and one can start the procedure of rock permeability measurement with use of the technique, which is described in details in [Shmonov et al., 2011; Malkovsky et al., 2013].

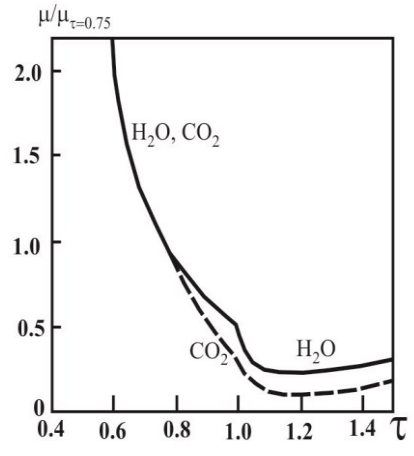

Fig.1. Dependence of dynamic viscosity on reduced temperature for water and carbon dioxide at $\pi = 1.1$.

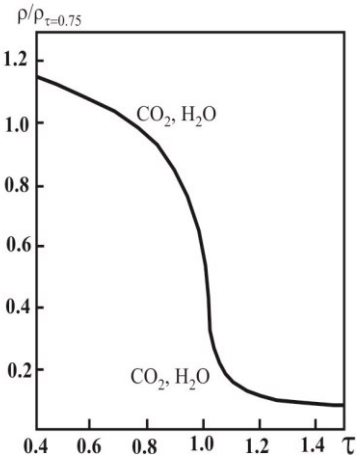

Fig.2. Dependence of density on reduced temperature for water and carbon dioxide at $\pi = 1.1$.

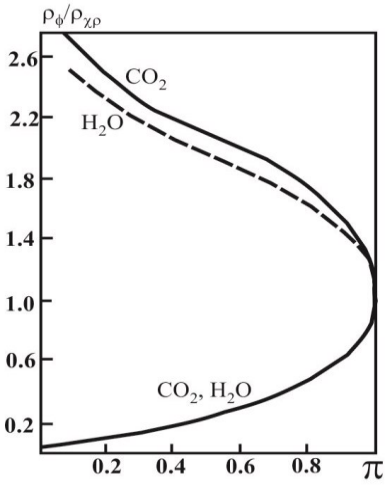

Fig.3. Dependence of liquid phase density on reduced pressure for water and carbon dioxide.

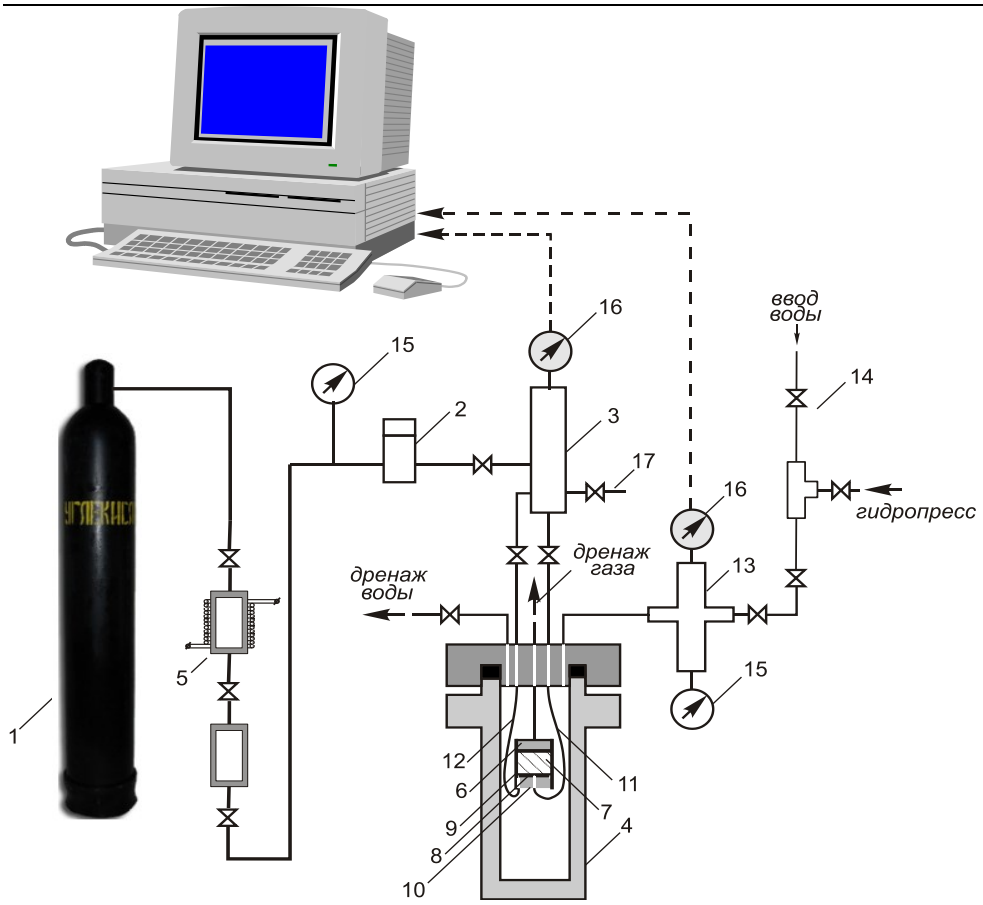

(1) gas-cylinder; (2) filter; (3) input volume; (4) high-pressure vessel; (5) thermal press; (6) output obturator; (7) sample; (8) tight joint; (9) side-wall isolation of the sample; (10) input obturator; (11–12) input of carbon dioxide; (13) manometer insert; (14) hydropress; (15) pointer manometer; (16) piezosensor for pressure; (17) branch for measurement of high permeabilities.

Fig. 4. Schematic diagram of apparatus for permeability measurement with use of carbon dioxide at near-critical parameters of state.

Schematic diagram of apparatus for sample permeability measurements for CO_2 is presented in Fig.4. A substantial difference of the diagrams in Fig.4 and in [Malkovsky et al., 2013] is presence of the thermal press for carbon dioxide. This is due to the fact that at subcritical temperatures ($T_{cr} \cong 304.2$ K) carbon dioxide in the cylinder is contained in a two-phase state (liquid+gas). As a result, the pressure in the gas-cylinder is equal to the pressure of saturated vapor of CO_2 p_{sat} at the temperature of environment T_0. If the first 4 valves between the gas-cylinder (1) and after the input volume are open, liquid CO_2 flows from the gas-cylinder into the input volume at the pressure of $p_{sat}(T_0)$. If it is necessary to study permeability of the sample for the fluid of supercritical parameters of the state, the pressure in the input volume (3) should be increased at least up to p_{cr}. This is fulfilled as follows. The liquid carbon dioxide flows from the gas-cylinder under the action of pressure in it and fills the volume of the thermal press (5) and the receiver placed below.

Dependence between p_c and T_1 is determined as follows. The mass of liquid CO_2 which flows initially from the gas-cylinder into apparatus, is equal to

$$m = \rho'(p_{sat}(T_0), T_0)(V_1 + V_2),$$

where $\rho'(p,T)$ is density of the liquid phase of CO_2 at the pressure p and temperature T.

The value of p_c is obtained through solution of the equation

$$\rho'(p_c, T_1)V_1 + \rho'(p_c, T_0)V_2 = m \qquad (1)$$

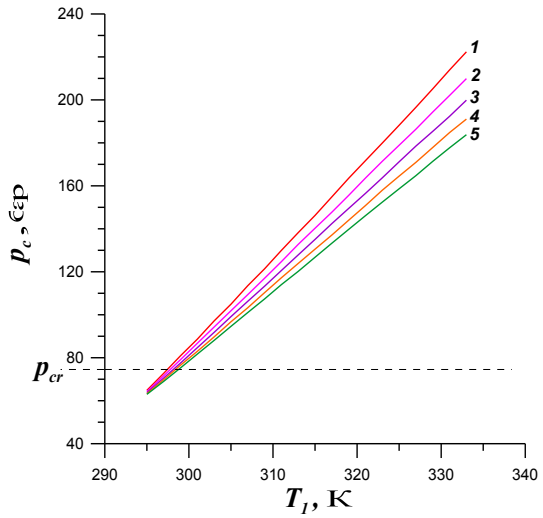

Fig. 5. Dependences of pressure in the receiver on temperature in the thermal press. (1) r=0.1; (2) - 0.2; (3) - 0.3; (4) - 0.4; (5) - 0.5.

The nonlinear equation (1) is solved numerically by the dichotomy method. The function $\rho'(p,T)$ is determined through approximating formulas from [Altunin, 1975].

The determined plots $p_c(T_1)$ at different $r = V_2 / V_1$ from 0.1 to 0.5 are presented in Fig.5

One can indicate that the supercritical pressure in the receiver can be obtained at relatively low heating of thermal press.

The work was performed within the framework of the research plan of IGEM and with the financial support of RFBR (grant No. 19-05-00466).

References:

Collins R.E. (1961) Flow of fluids through porous materials. New York: *Reinhold Pub. Corp.* 270 p.

Miropolsky Z.L., Soziev R.I. (1990) Fluid dynamics and heat transfer in superconducting equipment. New York: *Hemisphere Pub. Corp.* 315 p.

Malkovsky V.I., Zharikov A.V., Shmonov V.M. (2013) Use of Argon for measurement of rock permeability. *Argon. Production, characteristics and applications.* Ed. by Bogos Nubar Sismanoglu, Homero Santiago Maciel, Marija Radmilovec-Radjenovic, Rodrigo Savio Pessoa. N.Y.: Nova Science Publishers. P. 17–36.

Shmonov V.M., V.M. Vitovtova, A.V. Zharikov (2002) Fluid permeability of the rocks from the Earth crust. - Moscow: *Nauchniy Mir*. 216 p. (in Russian).